NTNU

Norwegian University of
Science and Technology

The susceptibility of grade 70 anchor chain steel to HISC

Knut Ove Dahle

Materials Technology

Submission date: July 2011

Supervisor: Jan Ketil Solberg, IMTE

Co-supervisor: Roy Johnsen, IPM

Norwegian University of Science and Technology
Department of Materials Science and Engineering

Preface

This master project was conducted at the Norges Teknisk-Naturvitenskaplige Universitet (NTNU) at the institute of materials technology in Trondheim in the spring of 2011. The work was carried out in cooperation with Erling Haug AS and Kjettingfabrikken. A special thank is given to lab engineer Nils Inge Nilsen for being so helpful in the Sintef Corrosion Lab at Perleporten. Also I would like to thank Ferrozink Trondheim AS for letting me use their hot dip galvanizing facility free of charge.

I would like to show my appreciation for the supervision and help I received from Professor Jan Ketil Solberg and Professor Roy Johnsen during my project work. I thank you for all the guidance and good advice you have given me.

Trondheim
Juni 2011

_____

Knut Ove Dahle

Abstract

Due to recent fractures in grade 70 anchor chains in the fish farming industry, chain supplier Erling Haug AS has initiated an examination of a sandblasted anchor they sell today. The sandblasted anchor chain is of the same strength category as the chains associated with the mentioned accidents. The mechanical properties of the sandblasted chain were characterized in 2010 in a student project work[1]. The report expressed concern about the sandblasted grade 70 chains since the material fulfilled requirements to be susceptible to hydrogen induced stress cracking (HISC). Therefore, further research on the material was needed. Another grade 70 chain, of an unknown origin, was obtained to make a comparison. This chain had fractured in-service. It was therefore necessary to characterize the mechanical properties of the fractured chain before examining the two chain grades susceptibility to HISC. The fractured chain was examined in terms of its microstructure, hardness, transition temperature and strength. An attempt was made to explain why the fractured chain failed in-service.

The tensile test of the fractured chain revealed that its yield strength was 140MPa lower than that of the sandblasted chain. It was considered possible that the fracture chain were weaker than they should have been and that the reason it failed in-service was due to overload.

The susceptibility of the two chains to HISC was tested by submerging tensile specimens into a 3.5% NaCl solution in CorTest Proof rings, while exposed to hydrogen. Specimens were either hot dip galvanized (HDG), protected by an external potential of -1050mV vs. Ag/AgCl or freely exposed at their corrosion potential. Some specimens were pulled in steps till fracture, while others were held at a constant load for 14 days.

Different loading and corrosion potentials were applied to the two chain qualities during the HISC test, but the experiment was unable to provoke brittle fractures in either of them. No cracking was observed in the SEM

for any of the HDG tensile specimens. It was found that hydrogen have no influence the mechanical properties of the HDG tensile specimens, while hydrogen appear to assist in the development of cracks on the polarized specimens.

Nomenclature

Ag/AgCl	-	Silver, silver chloride-electrode
BCC	-	Body Centered Cubic
BCT	-	Body Centered Tetragonal
Chain link	-	A link of several chain rings
Chain ring	-	One closed piece
CP	-	Cathodic Protection
HDG	-	Hot-Dip Galvanized
HE	-	Hydrogen Embrittlement
HEDE	-	Hydrogen Enhanced Decohesion
HELP	-	Hydrogen Enhanced Local Plasticity
HIC	-	Hydrogen Induced Cracking
HISC	-	Hydrogen Induced Stress Corrosion
HSC	-	Hydrogen Stress Cracking
SCC	-	Stress Corrosion Cracking
SCE	-	Saturated Calomel Electrode
SEM	-	Scanning Electron Microscope
SHE	-	Standard Hydrogen Electrode
$\sigma_{Y,F}$	-	Yield strength of the fractured chain
$\sigma_{F,F}$	-	Tensile strength of the fractured chain
$\sigma_{Y,S}$	-	Yield strength of the sandblasted chain
$\sigma_{F,S}$	-	Tensile strength of the sandblasted chain

Table of Content

1 Introduction

Recently several anchor chains used in the fishing industry have fractured[2]. The fractures of these anchor chains have had a catastrophic result where entire nets have failed and domesticated salmon have escaped. Such accidents not only cause large economic losses for the fish farming companies, but domesticated salmon also mates with wild salmon and spread diseases that threaten the survival of the wild salmon in several lakes along the Norwegian coast. In order to reduce the number of escaped salmon the industry is now focusing on improving the safety and reliability of the fishing facilities. As a part in this effort anchor chains being sold today are going through a quality check. Particular attention is directed at 16mm thick anchoring chains with the strength grade 70, because most of the recent fractures have been associated with this class.

Chain supplier Erling Haug AS, and chain manufacturer FRAM Kjettingfabrikken AS, are now cooperating with NTNU in order to investigate their strongest 16mm grade 70 anchor chain. Even though no anchor chains manufactured by Kjettingfabrikken AS have been reported to have failed in-service, their motivation have been to double check the quality of their product by testing it against possible failure mechanisms believed to cause the fractures in the mentioned chains.

In September 2009 Force Technology AS examined a fractured anchor chain, on behalf of the Norwegian Fishing Ministry, and found that it had fractured in a brittle manner[3]. A series of theories were put forward in an attempt to explain why the anchor chains had failed. One of the theories was that the chains were embrittled by hydrogen introduced during the acid pickling cleaning process prior to HDG. HDG is a common corrosion protection method used on anchor chains and is called cathodic protection (CP). It was decided to use this as a starting point when investigating the chains sold by Erling Haug. This theory was tested and disregarded after a study by Dahle [1] in 2010. In the study two

unused grade 70 chains with different cleaning methods prior to HDG were characterized and compared. The study revealed that insufficient amounts of hydrogen were introduced in the examined acid pickled chains to embrittle the material. The study also concluded that the chains fulfilled the requirements to be susceptible to induced stress cracking (HISC).

Force technology presented another theory to explain why the anchor chains failed in-service. It was belied that the chains had failed due to HISC, as a consequence of hydrogen introduced from CP. This theory was worth testing on the sandblasted chains as well since the material was found to be receptive to HISC. The main focus of this project work will therefore concern the susceptibility of the sandblasted grade 70 chains to CP induced HISC.

For that reason the discussion will encircle the mechanical properties of the HDG, martensittic type carbon steel used in anchor chains and how they are influenced by hydrogen. A constant load tensile test in seawater was executed in order to attempt to create a realistic scenario for the chain. The tensile specimens were exposed to hydrogen at different potentials to see how hydrogen would influence the mechanical properties of the steels, and if they would influence the materials resistance to HISC. If specimens failed, their fracture surfaces would be characterized in a scanning electron microscope (SEM) in order to verify if the samples showed a characteristic brittle fracture indicating hydrogen embrittlement or not.

In addition to the sandblasted chain, a chain of an unknown origin which fractured in-service was acquired. This chain was compared to the sandblasted chain with regards to its reaction to hydrogen exposure. First, it was necessary to characterize the mechanical properties of the unknown steel. Properties such as its transition temperature, tensile strength, microstructure and hardness were examined. After the

material was characterized it was subjected to a constant load tensile test in simulated seawater, as done to the sandblasted steel.

A secondary goal of this report was to reveal if there were any similarities between the fractured anchor chains and the unused sandblasted anchor chain. By examining the fractured chain it could be possible to find the reason for why it had failed. Both chains under examinations are of the highest strength class currently allowed in the fishing industry.

In order to understand the concept of HISC a broad theoretical background about factors involved in the phenomena is presented. This includes explanations of cathodic protection, diffusion mechanisms, fracture mechanisms and characteristics found in fracture surfaces related HISC.

2 Theory

In this section of the report attention will be given to educate the reader to understand the problem at hand. HISC is a subgroup under hydrogen embrittlement (HE)[4]. In order to comprehend the dangers regarding HISC, the background theory behind hydrogen embrittlement will be given before going more in depth on HISC. As an introduction some results obtained from previous experiments conducted on the anchor chains in question will be presented. Secondly, the effect of galvanic corrosion and corrosion protection will be explained. The next chapters will contain information about hydrogen embrittlement and the mechanism and role of diffusion. Chapter 2.5 will contain information about fracture mechanisms in metals. The final chapter will contain information about how one can recognize the fracture surface of a part which has failed because of hydrogen embrittlement.

2.1 Previous work

Another project work on the field was conducted in the autumn 2010[1]. That work focused on characterizing the properties of the sandblasted steel, and an acid pickled steel, used in anchoring applications. A comparison was made between the sandblasted chain and the acid picked chain. The report attempted to determine whether there was any difference between the mechanical properties of the steels due to the cleaning method prior to the HDG and if the pickling process could have embrittled the acid cleaned steel. The conclusions from the report[1] were that insufficient levels of hydrogen had been introduced into the steel during the acid pickling process to embrittle the metal, and that there were no significant difference in their mechanical properties. The acid pickling process was therefore reported acceptable.

Since the theory on an embrittling acid pickling process was rejected it was decided to do further testing on the sandblasted anchor chain. A second theory posted to explain the recent fractures in anchor chains were that they could fail due to CP induced HISC. Hence, the

sandblasted chain would be tested for their susceptibility to CP induced HISC. The mechanical properties of the sandblasted steel can be found in Appendix A – Previous work, and are relevant for this project.

2.2 Cathodic protection of steel in seawater

When a steel structure is submerged in seawater it needs to be protected against corrosion in order for the construction to maintain its function. One way to maintain the constructions function is by applying a cathodic protection. The main principle behind cathodic protection is to protect a substrate by supplying an external current so that the electrode potential of the material being protected is pushed down into its immune area or below a protection potential in the Pourbaix diagram. The Pourbaix diagram gives the connection between the electrochemical potential E, the solutions pH and the condition of the metal (corrosion, passive or immune) as shown in Figure 1.

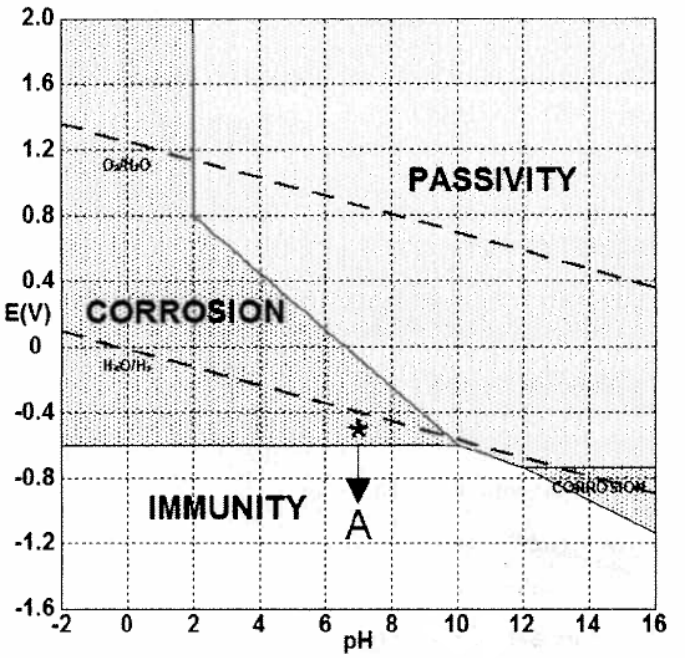

Figure 1. Pourbaix diagram for carbon steel in tap water with pH 7 vs. standard hydrogen electrode[5].

The material in question is consequently turned into the cathode in an electrochemical cell, which is being polarized cathodically as illustrated in the potential- log current curve displayed in Figure 2. This kind of corrosion protection is called CP, and is based upon the principle of galvanic corrosion[6].

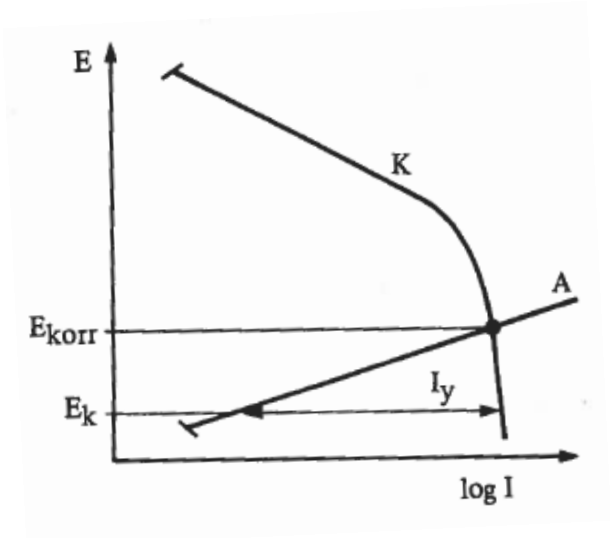

Figure 2. Shifting of potential from the free corrosion potential E_{corr} to a lower potential E_k by aid from an external current I_y[6].

The external current I_y is the difference between the cathodic and the anodic current at the actual potential E_k. With corrosion protection the anodic current on the protected material is equal to 0 or relatively small, so the external current is almost equal to the cathodic current[6].

An external current can be used to polarize the steel cathodically in three different ways. Firstly, one can attach sacrificial anodes made from a less noble material than the material which is being protected. Secondly, one can use an external power source such as a rectifier. Alternatively, one can apply a coating less noble than steel, which is the corrosion protection normally used on anchor chains. The most commonly used anodic coating is zinc. An anodic coating protects the steel in three different ways;

i. The barrier effect blocks the corrosive media from coming into contact with the material which is protected.
ii. It functions as a CP where zinc sacrifices itself to protect the steel.
iii. Inhibition and passivization, including instances of anodic protection.

If the zinc coating is damaged a favorable area relationship between the anode and the cathode gives a low corrosion rate on the zinc coating. The cathodic reduction of water can then occur for pH < 8 – 9, without CO_2;

Reduction reactions:

$$2H^+ + 2e^- \rightarrow H_2 \quad (1)$$

$$O_2 + 2H_20 + 4e^- \rightarrow 4OH^- \quad (2)$$

A potential danger related to this is HE. HE is a detrimental consequence of the hydrogen evolution from the cathodic reaction. The risk of HE is especially high when high tensile stresses and materials with high material yield strength and hardness is involved[6]. More information about this phenomenon will be given in the next chapter.

2.3 Hydrogen embrittlement and HISC

Damage resulting from hydrogen being entrapped in materials in use has been a problem for a number of years. The phenomenon is primarily associated with ferritic (BCC) materials, particularly high strength steels, but has also been known to occur in martensittic (BCT) materials. The damages may present themselves in a number of forms, such as internal flakes or “fish eyes” surrounded by ductile fracture, cracks or general embrittlement, which results in premature failure[7].

Definitions

Before going into further details about how HE works, some terms needs to be defined. In the theory there exist several types of hydrogen embrittlement depending on the origin of the hydrogen and if the part is under and form of stress. According to the standard *ISO 21457:2010 - Materials selection and corrosion control for oil and gas production system* one mainly refers to hydrogen-induced cracking (HIC) or hydrogen stress cracking (HSC)[4]. HIC is more commonly referred to as HE and is defined *as "planar cracking that occurs in carbon and low alloy steel when atomic hydrogen diffuses into the steel and then combines to form molecular hydrogen at trap sites".* As further explained, cracking results from hydrogen atoms that recombine into gas and apply pressure at trap sites. No externally applied stresses are needed for the formation of hydrogen-induced cracks. Typically, trap sites capable of causing HE is normally found in steels with high level of impurities. Such impurities are most commonly planar inclusions or regions of abnormal microstructure produced by segregations of impurities and alloying elements in the steel. This type of hydrogen induced cracking is normally not related to welding. As the case is for the anchor chains, no cracking has been observed to occur at the welded part[4].

HSC, or more commonly referred to as HISC (hydrogen induced stress cracking), is defined *as "cracking that results from the presence of hydrogen in a metal and tensile stress (residual or applied)".* For simplicities, only the term HISC will be used because chains are normally under tension stresses in use and the influence of hydrogen generated from CP is the phenomena under examination. Furthermore, the standard emphasizes that *"HISC describes cracking in metals that are not sensitive to stress corrosion cracking (SCC) but which can be embrittled by hydrogen when coupled galvanically, as a cathode, to another metal that is actively corroding, e.g. zinc*"[4].

Sources of hydrogen

The origin of the embrittling hydrogen can vary. It can either come from the manufacturing process of the part or it can be introduced into the material while it is in-service. According to Colangelo[7] a major source of hydrogen is from the steel melt when water is reacting at high temperatures with the liquid iron. The water vapour may come from the scrap used to change the furnace, the slag ingredients or from the refractory materials lining the furnace. The resulting hydrogen may become trapped during solidification as solubility decrease. Hydrogen may also become available during acid pickling or plating operations prior to e.g. HDG.

Exposure during the parts service lifetime to process fluids containing hydrogen, as in catalytic cracking, can also cause embrittlement. Similarly, hydrogen may be generated as a corrosion product in certain environments, as discussed in chapter 2.2, and thereby become available to cause embrittlement. In welding, the principal source of hydrogen is moisture in the electrode coating or humidity in the atmosphere. High strength steels are difficult to melt during conditions of high humidity because of hydrogen pick up. Consequently, these steels are vacuum degassed prior to pouring to remove the hydrogen.

HISC under CP

The three necessary components for hydrogen embrittlement to occur is thus a susceptible material, in a hydrogen rich environment under stresses[8]. For martensittic carbon, low-alloy steels, failures by CP induced HISC have been encountered involving materials with an actual YS and hardness of about 700 MPa and 350 HV, respectively. It is widely recognized that untempered martensite is particularly prone to HISC[9].

When carbon steel is under CP and corrodes, the zinc coating will give off electrons and protect the steel. If the zinc coating is damaged, the electrons can be transported to the steel surface and release hydrogen atoms there. These electrons will react with the environment and

generate hydrogen as a corrosion product, according to the equations in chapter 2.2. This hydrogen can then be absorbed into the metal[5].

For carbon steel in seawater the normal corrosion potential E_{corr} is in the range of -550 to -600 mV vs. Ag/AgCl. To protect the carbon steel from corrosion a potential of $E_p \leq$ -800 mV vs. Ag/AgCl is normally required[5].

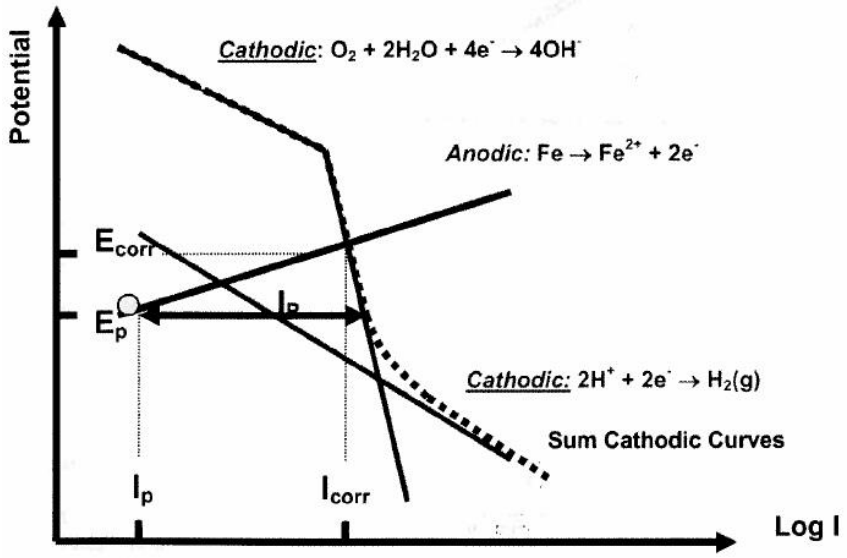

Figure 3. Evans diagram for steel in seawater with protection current I_p included[5].

Figure 2 shows the *E*-log*i* curve for carbon steel in seawater with an impressed cathodic current I_P. As can be seen from the figure the external current lowers the potential of the steel and consequently reducing the anodic dissolution of iron[5]. Figure 2 also shows that the hydrogen reaction becomes more and more dominant when the potential is lowered. Hence, the more hydrogen is anticipated to be developed when the steel is polarized to -1050mV vs. Ag/AgCl. This is the main reason why it is important to restrict the minimum potential on steels that can suffer from HISC.

Hydrogen reactions

The electrochemical based adsorption mechanism works in such a way that hydrated hydrogen cations H_30^+, are transported towards the cathode where it they are reduced and become atomic hydrogen H. This atomic hydrogen can consequently recombine and form gaseous hydrogen molecules, which can either leave the surface or be absorbed into the subsurface of the steel instead. Two types of reaction mechanisms follow the reduction of hydrated hydrogen:

A. <u>The Volmer – Tafel mechanism</u> is based on an electrochemical reaction were hydrated hydrogen atoms are reduced to atom hydrogen by taking up an electron and being adsorbed in on the metal surface. In the second step of the reaction, two adsorbed atomic hydrogen atoms recombines and form molecular hydrogen gas.

$H^+_{hydrated} + e^- \rightarrow H_{adsorbed}$	Volmer	(3)
$H_{adsorbed} + H_{adsorbed} \rightarrow H_2$	Tafel	(4)

B. <u>The Volmer – Heyrovsky mechanism</u> is based on the same initial reaction, but is followed by a different electrochemical reaction were another hydrated cation is reduced with a hydrogen atom already adsorbed on the metals surface, and forms molecular hydrogen. The rate of this reaction depends on the potential in relations to the cathodic protection, where protection potentials below -800 mV vs. Ag/AgCl will start producing hydrogen[8].

$H^+_{hydrated} + e^- \rightarrow H_{adsorbed}$	Volmer	(3)
$H^+_{hydrated} + H_{adsorbed} + e^- \rightarrow H_2$	Heyrovsky	(5)

The potential, below which the hydrogen reduction reaction can occur, can be found by equation 6[6]:

$$E_0 = E_0^0 - \frac{2.3 \cdot R \cdot T}{z \cdot F} \cdot log \frac{1}{[H+]^2} \quad (6)$$

Here, E_0 is the equilibrium potential for the hydrogen reduction. $E_0{}^0$ is the standard electrode potential for the reaction at 25°C. *z* is the number electrons transferred in the reaction. $[H^+]$ is the concentration of H^+ atoms in the solution. The hydrogen concentration is found from the function $[H^+] = 10^{-pH}$. R is the gas constant 8.3 Joule/K·mol. F is the faraday constant 96 485 C/mol[6].

Theory behind HISC

Hydrogen atoms produced electrochemically can be adsorbed at a crack tip, as seen in Figure 4. Some of the adsorbed atoms penetrate the metal at the crack tip. These can diffuse ahead of the crack tip as a result of enhanced diffusivity in the plastic zone. Thus, an embrittled zone is created ahead of the crack tip which enhances the growth of an intercrystalline or a transgranular crack, the latter by a cleavage- type mechanism[10]. These cracking phenomena are explained in more detail in chapter 0.

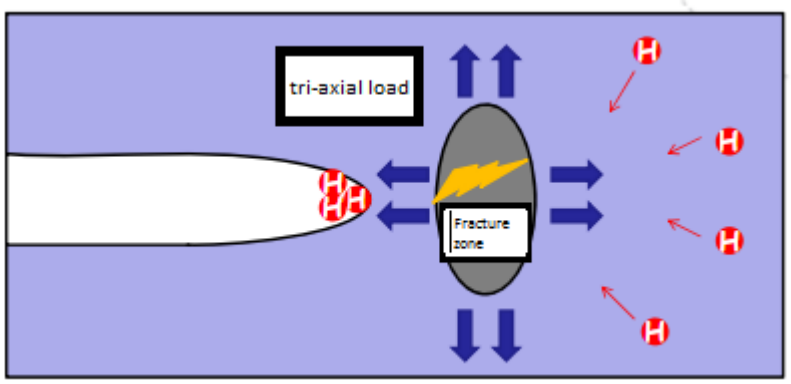

Figure 4. Diffusion of hydrogen near the tri-axial stresses at the crack tip[5].

The effect of local stress and strain fields on the hydrogen diffusion is especially interesting due to its effect on the metals mechanical properties and fracture toughness. A notch or crack subjected to a plane opening stress is described by a local stress and strain field ahead of the notch tip. The strain field is at its highest at the notch tip and then gradually decreases with increasing distance from the notch tip. The hydrostatic stress field reaches a maximum a short distance ahead of the crack tip, as seen in Figure 5. The diffusible lattice hydrogen will accumulate at sites of increased hydrostatic stress due to dilatation of the lattice. Hydrogen also accumulates at trapping sites caused by local plastic deformation[11].

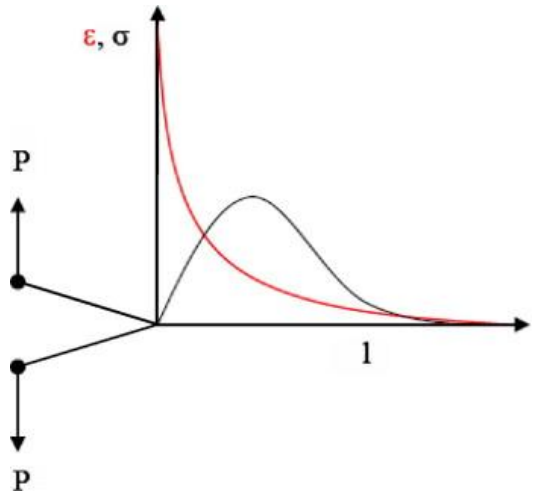

Figure 5. Illustration of stress and strain field in HEDE ahead of a notch tip in plane mode I loading[11].

In bcc metals, such as martensittic steel (BCT), typical trapping sites for atomic hydrogen and molecular hydrogen are structural defects as;

- Dislocations
- Atoms in solution
- Vacancies
- Grain boundaries
- Particle interfaces
- Microcracks and pores[12].

Two of the most cited theories for explaining HE is called *hydrogen enhanced decohesion* (HEDE) and hydrogen *enhanced local plasticity* (HELP). The HEDE mechanism is based on the hypothesis that interstitial hydrogen lowers the cohesive strength by dilatation of the atomic lattice and hence lowers the fracture energy. This implies that hydrogen decreases the energy barrier for either grain boundary or cleavage plane decohesion. The notion is that fracture will initiate in the area of maximum hydrostatic stresses some distance ahead of the crack tip.

HELP is characterized by atomic hydrogen enhancing the mobility of dislocation movement in preferred crystallographic planes at the crack tip. The propagation of the crack is illustrated in Figure 8. This local softening results in cracking by micro void coalescence along these planes. The mechanism can be describes as local plasticity that is macroscopically brittle. A HELP crack will tend to initiate from slip planes in the crack tip, as illustrated in Figure 6 [11].

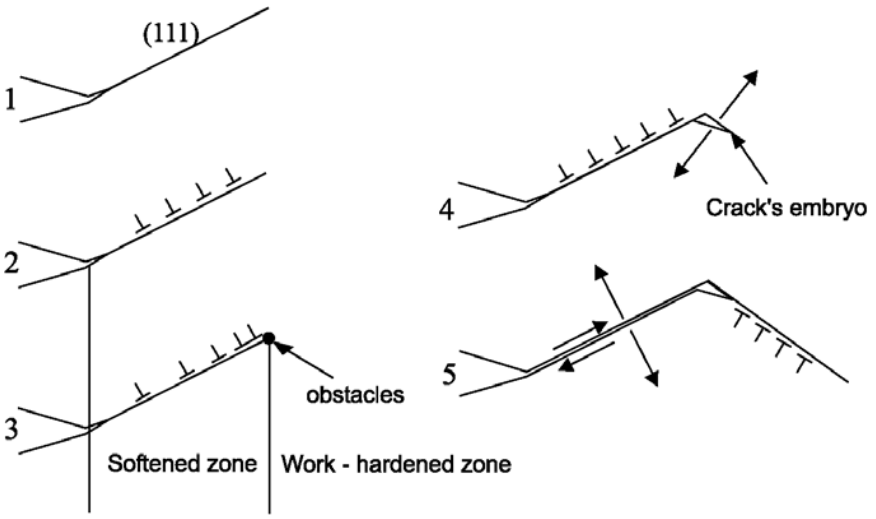

Figure 6. Successive steps in hydrogen enhanced local plasticity, HELP: 1) slip planes activated at the crack tip, 2) enhanced plasticity on (111) planes due to hydrogen adsorption, 3) pile up of dislocations near obstacle, 4) initiation of crack or micro void due to the local stress increase and 5) the crack opens by shear decohesion along the plane[11].

In a situation with increased hydrogen concentration in the crack tip it is clear that the crack propagation is promoted by whether is by HEDE or the HELP mechanism. In that sense it can be argued that the crack tip response to stress under hydrogen influence is a competition between atomic lattice decohesion and dislocation emission, between brittle and ductile response, but at a lower (local) stress level than without hydrogen influence[11].

2.4 Diffusion

Diffusion refers to the net flux of any species, such as ions, electrons, holes, atoms and molecules. The magnitude of the flux depends upon the initial concentration gradient and temperature. In order to diffuse the atom must squeeze past the surrounding atoms to reach a new site[13]. There are several mechanisms for atoms to diffuse, but this report will mainly focus on the mechanism relevant for hydrogen to diffuse in steel.

Lattice diffusion by interstitial jumps is the main diffusion mechanism for hydrogen in steel[11]. A ferritic base centred cubic (bcc) structure enables a high diffusion rate and a low solubility due to its open lattice structure. In contrast, the austenitic phase centred cubic (fcc) structure gives a lower diffusion rate and a higher solubility due to its close packed lattice. Martensite is basically body centred tetragonal (btc), but a tendency towards hexagonal martensite formation (hcp) increases with the carbon content. These structures are closer packed than bcc. As a result the diffusion rate of hydrogen in martensite is between ferrite and austenite[11]. The lattice diffusion coefficient D can be described by the relation of the Arrhenius form:

$$D = D_0 \exp\left(-\frac{E}{RT}\right), \qquad (7)$$

Where E is the activation energy (J/mol) and R is the gas constant (8,314J/molK) and T is the temperature in Kelvin. Reported values for D_0 is in the range of 0.076 – 0.22 mm^2/s for ferrite and in the range of 1.1 – 1.5 mm^2/s for austenite. The related activation energy for lattice diffusion in given as 12.5 J/mol for ferrite and about 42 J/mol for austenite.

Fick's first law describes the diffusion of hydrogen (the flux of hydrogen atoms) from a region with high concentration to one with low concentration:

$$J_x = - D \cdot (\Delta C)_t, \qquad (8)$$

$(\Delta C)_t$ is the concentration gradient at a specific time t[11].

2.5 Fracture mechanisms in metals

In this section attention will be given to the most common fracture mechanics found in metallic materials and alloys. Later in the report one will find pictures of fracture surfaces, and it will therefore be necessary to explain how the fracture surface characteristics can be recognized and how they got there. A metallic material can mainly fracture in three different ways. The main fracture mechanisms are ductile fracture, cleavage fractures and brittle fractures, where cleavage fractures is a large subclass to brittle fractures. A forth mechanism called fatigue also exists, but it will not be mentioned here because it is unrelated to the topic of this reports [14].

2.5.1 Ductile fracture

In ductile fractures the crack propagation normally occurs in a transgranular manner, meaning though the grains, which have good ductility and toughness, as shown in Figure 7. For this kind of fractures one can often observe considerable deformation, such as necking, in the failed component. The deformation occurs before the final fracture. Overloading or applying too high stresses to a component are usually the most common reasons for a ductile fracture[13].

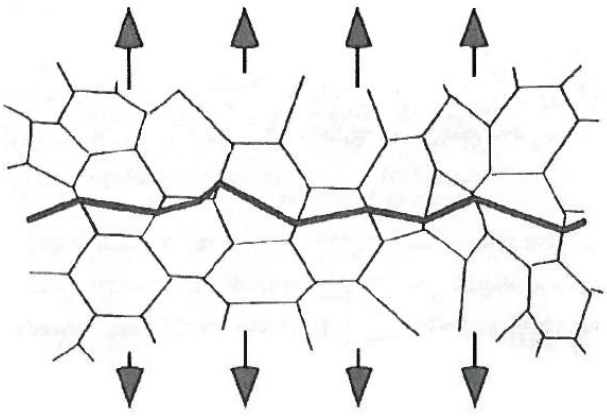

Figure 7. Crack propagation in a transgranular fracture[14].

In a tensile test, ductile fracture initiates with the nucleation, growth and coalescence of micro-voids at the centre of the tensile specimen, see Figure 8. High stresses causes separation of the metal and micro voids nucleate at grain boundaries or at interfaces such as impurities and inclusions. As local stresses increases, the micro voids grow and coalesce into larger cavities. Ultimately, the metal-to-metal contact area will be too small to support the load and fracture occurs[13].

During ductile fracture of a metal deformation can also occur as slip. Slip may occur when the resolved shear stress reaches the critical resolved shear stress and the stresses are highest at a 45 degree angle to the applied tensile stress [13].

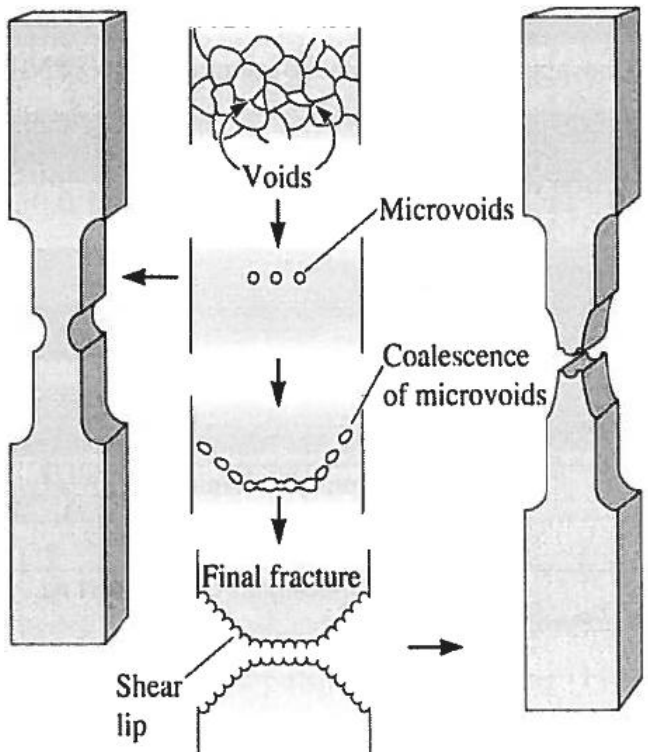

Figure 8. In a tensile test, when a ductile material is being pulled, necking begins and voids start to form near the center of the bar by nucleating at grain boundaries or inclusions. As deformation continues a 45 degrees shear lip may form to produce a final cup and cone fracture[13].

A ductile fracture gives the fracture surface a characteristic look. In thick metal parts, one can find evidence of necking, with a substantial part of the fracture surface having a flat face. There, the micro voids will nucleate and coalesced, and a small shear lip will appear around the edges, with a 45 degree angle. The shear lip, indicates that slip has occurred, gives the fracture cup and cone appearance, as displayed in Figure 9. Macroscopic observation of this kind of fracture characteristics may be sufficient to identify the ductile fracture mode[13].

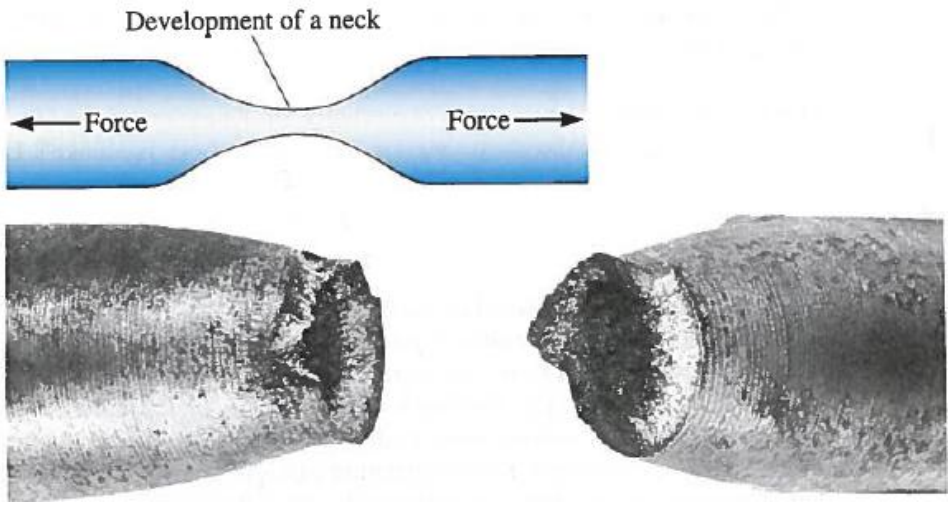

Figure 9. Localized deformation of a ductile material during a tensile test produces a necked region. The bottom image shows a necked region in a fractued sample, with a typical cup and cone shape[13].

In Figure 10 a fracture surface is examined at a high magnification, and one can observe dimples. Dimples are signs of microvoids produced during the fracture. These are normally equiaxed when normal tensile stress produces the failure. On the shear lip however, they may appear as ovals and will point towards the origin of the fracture.

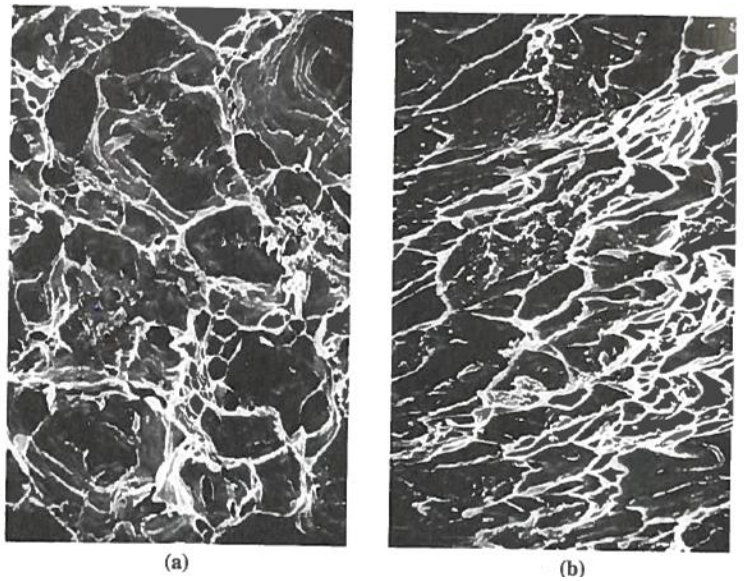

Figure 10. Fractographic images at 1250x of an annealed 1018 steel exibiting ductile fracture in a tensile test. a) equiaxed dimples aft the flat center of the cup and cone, and b) elongated dimples at the shear lip[13].

In a thin plan subjected to tensile stresses, less necking is observed. Here, the entire fracture surface may be a shear face. Examinations of the fracture surface in a microscope normally show elongated dimples rather than equiaxed dimples. This indicates that a greater part of the fracture surface fail due to 45 degree compared to thicker metal parts[13].

2.5.2 Brittle fracture

Brittle fracture is a failure mechanism that is normally associated with high strength metal and alloys with poor ductility and toughness. Even ductile metals may fail in a brittle manner at low temperatures, in thick sections and at high strain rates, such as impact, or when flaws play an important role. There could be many reasons for why the ductility of a metal is reduced, but this report will only cover factors which are relevant to hydrogen embrittlement. Some of these factors were mentions in chapter 2.3. Brittle fractures are most common when impact, and not overload, causes failure[13]. Typical for brittle fractures

are little to no plastic deformation. These types of fractures can occur at stresses below the materials yield strength[7].

In brittle fractures, most energy goes into the fracture and creates the surface. Initiation of the crack normally occurs at notches, small surface cracks, small flaws or stress concentrations. The crack propagates most easily along certain crystallographic planes, typically in the [100] planes for BCC materials, by cleavage. The reason the preferred cleavage planes is the plane with the lowest packing density is due to the fact that fewer bonds must be broken there and the spacing between planes are greater. The crack may propagate in an intergranular path, along grain boundaries, particularly when segregations or inclusions reduce the strength of grain boundaries. An intergranular crack growth is shown in Figure 11 [14].

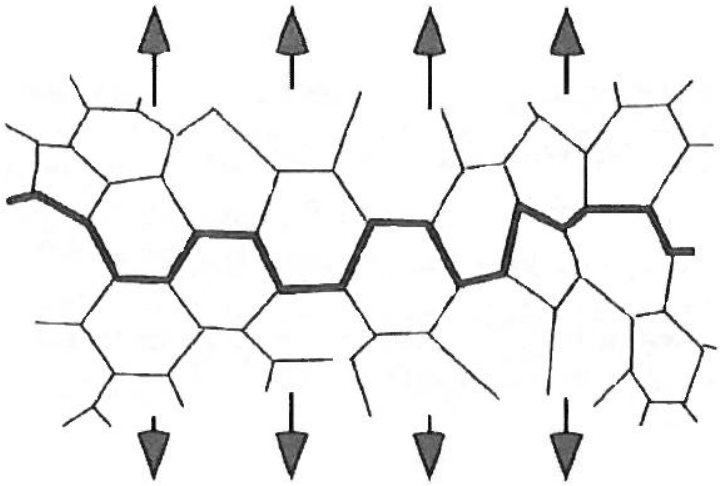

Figure 11. Inter- crystalline fracture. Crack propagation along grain boundaries[14].

By examining the features of a fracture surface one can determine if the part failed in a brittle fashion. The fracture surface is normally flat and perpendicular to the applied stress in a tensile test. If the failure occurs by cleavage, as shown in Figure 12, each of the fractured grains will be flat and differently oriented giving a crystalline appearance of the fracture surface[13]. Fractures may also appear without shear lips.

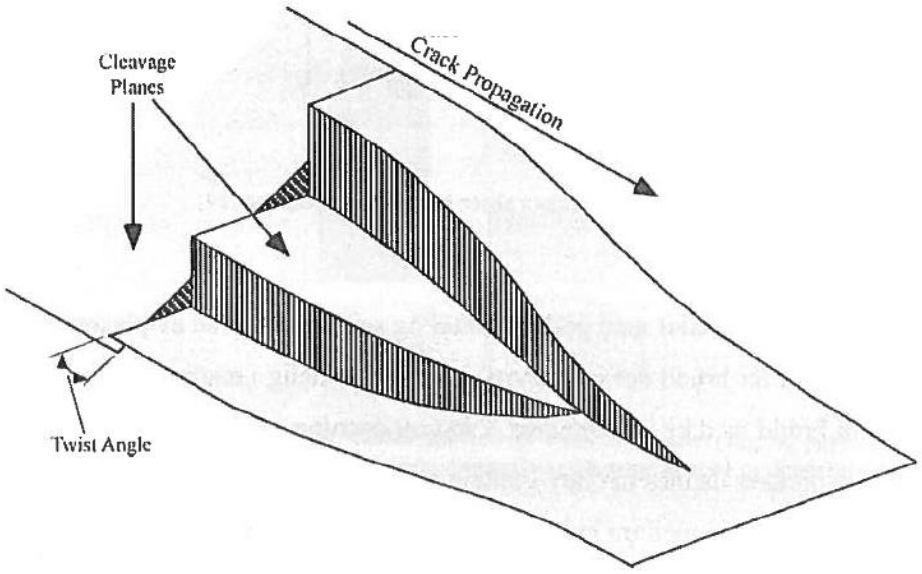

Figure 12. Formation of a river pattern due to a cleavage fracture. The cracks multiply and planes are cracked open[14].

Chevron patterns are also a common feature of brittle fracture, which is produced by separate crack fronts growing at different levels in the material. A radiating pattern of surface markings, or ridges, fans away from the crack initiation point[13].

2.6 Characteristics of hydrogen embrittled fracture surfaces

When looking after evidence of hydrogen damage in steel on the surface fractography, the visual features vary. Inside the material microcracks can initiate, often near inclusions or other interfaces, and propagate in an intergranular fashion for a certain distance. Inclusions play a significant role in hydrogen embrittlement. An inclusion acts as a hydrogen trap, and the concentration between the matrix and the inclusions interface therefore increases and facilitate cracking[7].

Cracks may also originate from electroplated surfaces. Although the cracked and micro cracked regions may fail in a brittle fashion the regions between the adjacent microcracks fail in a ductile manner and present evidences of dimpling. When the cross section of the specimen has been reduced sufficiently, the final load bearing will fail by overloading.

Typical characteristic of a hydrogen embrittled fractures can be difficult to distinguish from stress corrosion cracking (SCC) related fractures. Some of the main differences are;

- Hydrogen embrittled failures normally initiate below the surface, while in SCC they start at the surface.
- SCC fractures usually have more branches out from the main crack compared to HE cracks
- The initiation point is likely to be more corroded during SCC
- Fine markings, like hairline cracks are more pronounced by HE.

Fractures generated by hydrogen embrittlement could become corroded after cracking, but such can generally be seen by patches of rust on both intergranular or transgranular fracture by brittle cleavage or interface separation, depending on the relative strength of the grain-boundary[15].

3 Experimental

An objective of this project is to compare an unused sandblasted chain with a fractured chain in term of their susceptibility to HISC. A characterizing of the mechanical properties of the fractured chain was necessary before it was possible to evaluate the two chain qualities. A second goal with the report is to attempt to explain why the fractured chain failed in service.

Threaded tensile specimens are made from the two chain qualities for a HISC test. They are put into a CorTest Proof ring to test their resistance to cracking in a seawater environment under different corrosion conditions. The equipment and test procedure used is explained in detail in chapter 3.3.6.

In this section one can find information about the properties of the chain materials. There will also be a section showing the design of the anchor chains. Additionally, one can find information about how samples were selected and prepared for testing.

3.1 Materials

The sandblasted chain was produced by Kjettingfabrikken AS and delivered by supplier Erling Haug AS. The chains were unused, and delivered in three different packages. The sandblasted chains were delivered in 5 separate chain links. The 5 chain links had respectively 6, 10, 10, 11 and 32 rings each. It is unknown how the links were placed relative to each other from the original chain. It was said that all the chains came from the same shipment. It was unknown how long they had been on storage or where the steel came from. Their mechanical properties were examined and found in a project work executed during the autumn 2010[1]. Properties such as the materials microstructure, hardness, tensile strength and transition curve were found and are

presented in Appendix A – Previous work. The author of this report would like to emphasize that the results of the following experiments are only relevant when talking about the sandblasted chain of grade 70 delivered by Kjettingfabrikken. To say anything about grade 70 chains from other manufactures one need to perform similar tests on them.

The second examined chain quality in this project work is of an unknown origin. Unknown factures include how long the chain was in use prior to failing and were it was manufactured. The rings were unmarked and had no identification numbers of marking. The chain was said to be of grade 70, the same strength class as the sandblasted chain. Unfortunately, this could not be verified by any documentation. Its microstructure, hardness and tensile curve will be tested later in this report. The impact strength of the material will be found by the charpy test. The four rings of the fractured chain link were delivered as seen in Figure 13.

Figure 13. The link of the fractured chain steel as-delivered.

The strength term grade 70 needs to be explained. Grade 70 is in the industry label for the material or component strength. A grade 70 steel is also called grade 7, but for simplicity only the term grade 70 will be used in this report. Grade 70 refers to the materials nominal tension by a specified minimum fracture load of 700MPa (fracture load equals tensile strength). In this context it is important to distinguish between the yield strength/ tensile strength of the chain material and the yield strength/ tensile strength of the chain links. A grade 70 chain link will have a “minimum specified” fracture load of 700MPa. The “minimum specified”

fracture load of the chain link is not the same as the fracture load as the chain material.

The alloying elements of the sandblasted steel are given in Table 1, as presented in the material certificate. The composition of the sandblasted chain was not experimentally verified. As can be seen from the Table 1, the composition of the fractured material was not known. The sandblasted chain is of the highest allowed strength class grade 70. It was said that the fractured chain material was of the same strength class, but this has not been verified by any identification.

Table 1. Alloy elements of the sandblasted steel in wt%.

	C Ti	Si Cu	Mn Alt	P B	S N	Cr	Mo	Ni
Sandblasted, HDG steel	0.21 0.031	0.22 0.03	1.00 0,031	0.010 0,004	0.005 0,004	0.23	0.001	0.05

The material properties of the sandblasted steel are as mentioned presented in Appendix A – Previous work, but a summary is given in Table 2.

Table 2. Mechanical properties and coating thickness of the sandblasted steel.

	Sandblasted, galvanized steel
Yield Strength (MPa)	1030
Tensile strength (MPa)	1070
Elongation to fracture	≈ 13 %
Transition temperature	-11°C
Average hardness (HV)	367
HDG Coating thickness*	Min. 100 µm

*The value is as stated in the material certificate, and has not been experimentally tested.

The design and the dimensions of the chain rings under investigation are shown in Figure 14. The measurements of the chain rings are; L = 100 mm, B = 60 mm and D = 16 mm.

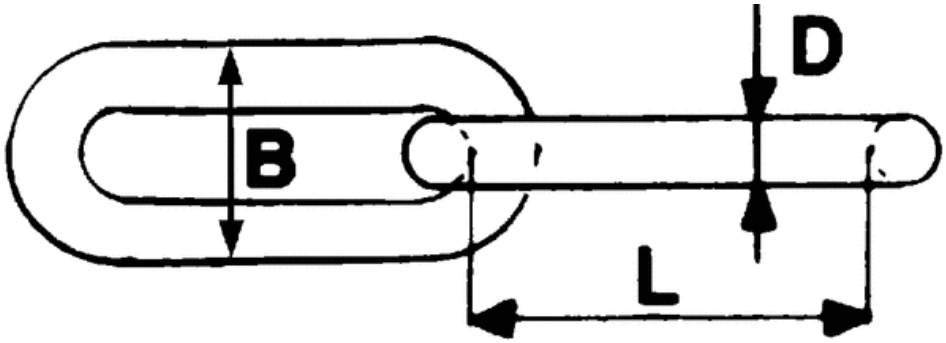

Figure 14. Design of the chain rings under examination[16].

The sandblasted chain came with a material certificate. In the certificate information about the materials yields strength and tensile strength could found. Several material properties were unfortunately missing. The certificate did not state which heat treatment the steel had been subjected to, the hardness of the steel, the transition temperature for the steel or which microstructure it has. This was therefore examined in the report from 2010[1].

3.2 Experimental program

Inclusions and structural defects play a significant role in hydrogen embrittlement it will be searched for in the light microscope and the scanning electron microscope. Inclusions acts as hydrogen traps and the concentration at the inclusion/matrix interface increases and facilitate cracking.

A hardness test was conducted to find the hardness of the fractured chain material. The measurements could be used to evaluate the homogeneity of the material in the chain link.

The charpy test was conducted to see if the transition temperature of the steel is suitable for its use. Because there were only four chain rings of the fractured material only two charpy specimens could be taken from the unwelded bar of the chain ring. Therefore, eight additional charpy specimens were taken from position III and IV according to Figure 6.

The ductility of the anchor chain was tested by performing a tensile test. Due to a lack of sample material only one tensile specimen was made out of the fractured anchor chain and pulled until fracture. The yield strength and tensile strength of the material would be found this way.

From the fractured chain and the sandblasted chain, 2 and 25 tensile specimens were prepared respectively. It was decided to conduct a constant load tensile test on the two chain materials in a CorTest Proof ring cell. The test was performed in 3.5% NaCl solution at room temperature.

Some specimens were pulled until fracture to find the materials fracture load under the test conditions, and some specimens were subjected to a constant loading at two different load levels for 14 days. Hydrogen will be introduced into the material at three different corrosion conditions. In the first condition the specimens are polarized at -1050mV vs.

Ag/AgCl. In the second condition the specimens are HDG were steel is exposed due to a simulated “damage” in the coating. In the third condition the tensile specimens are not protected from corrosion at all. The constant load test was carried out to see if the two steels could fail or crack due to hydrogen induced by the CP.The test program can be seen in detail in chapter 3.3.6.

The fracture surfaces from the tensile test were examined in a scanning electron microscope (SEM) in order to characterize if the specimens had failed in a ductile or brittle fashion. The specimens subjected to constant load for 14 days, which did not fracture, were examined in the SEM for microcracks on the specimen surface.

3.3 Apparatus and procedure

3.3.1 Light microscope

Examination in light microscopes was conducted on a Leica MeF4M with a Progress C10 digital camera. The samples were prepared by casting them in a Clarosit mould. Secondly the samples were grinded on 500µm, 1200µm and 2400µm cutting disks, respectively. Before examinations in the microscope, the samples were polished with 6, 3 and 1 grade polishing papers. Finally the samples were etched in a 2% nital solution for 6 seconds. The enlargement of the pictures was indicated with a scale bar.

3.3.2 Hardness testing

The tests were conducted on a DVK-1s-Matsuzawa hardness machine and measured in Vickers. The chain rings were cut out into samples with a Diskotom 5, by Struers. The cutting discs were of the type 50A24 and 60A25, also from Struers. The samples were then casted in Clarosit and consequently grinded on 800µm disks until even.

Since only 4 rings were obtained of the fractured chain most of the material was used to make charpy, tensile and threaded tensile specimens. Therefore, the hardness measurements were only conducted on left over pieces from the bend in the chain ring, according to position I marked in Figure 15. On basis of the results from 2010[1] this was considered to be a good approach because no hardness variations was found within each of the hardness tested chain rings in that report.

For the bend, hardness imprint number 1 was taken near the outside of the chain ring, while measurement number 5 was taken from the inside of the chain ring, as shown in Figure 15 b.

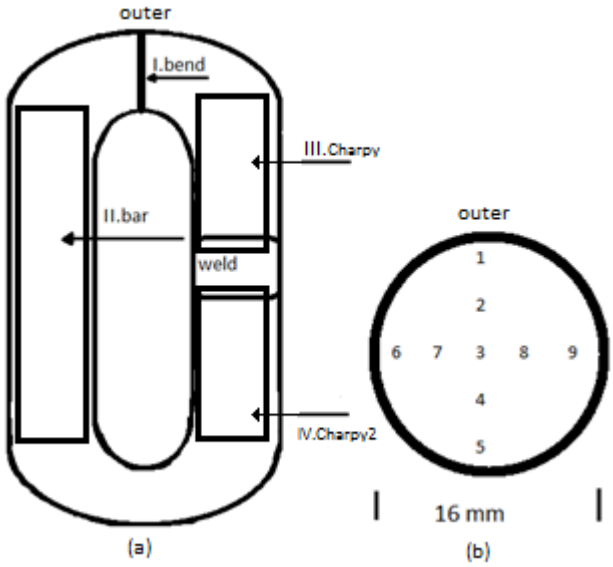

Figure 15. Picture of where the different test specimens were taken from in the chain ring. a) Shows a sketch of the chain ring and indicates where the specimens where taken from. The relative numbering of the hardness imprints done on the samples from position I (bend) is shown on figure b). Specimens for the HISC test and the charpy test were taken the sandblasted and the fractured chains from position II. Position III and IV shows where eight of the charpy specimens came from in the fractured chains.

A total of 9 hardness imprints were taken from each sample from the bend. A total of four casts were made from the bend and hardness tested with 9 imprints each, one from each of the four fractured chain rings. The hardness measurements were done in order to evaluate the homogeneity of the chain material and to determine the hardness.

Normally one can convert the results from the hardness test into other material properties. From table B.2 in ISO Standard 18265:2003 one can convert the hardness into tensile strength. This is a way to control the accuracy of the results of the performed tensile test.

3.3.3 Charpy test

By determining the transition temperature for ductile to brittle fracture for the fractured chain material, it would be possible to determine if the material was suitable for anchoring application or not. In order to get sufficient data to find the transition temperature it was necessary to machine out as many specimens as possible. With only 4 fractured chains, it was decided to make two test specimens from each side of the weld per chain ring and two additional specimens from the unwelded side of ring 1. This would add up to a total of 10 charpy specimens. How this was done can be seen in Figure 16, where the samples are taken from the welded side of the chain ring. As can be seen from the figure the samples will suffer from some minor material loss on the sample ends. The v-notch was machined on the surface facing into of the chain loop. According to the standard for charpy testing this is acceptable as long as the sample length is intact and the flats touching the sample bearing on the test equipment are correct.

Figure 16. The sketch shows the positioning of the charpy samples in the chain ring. Here from the welded side of the ring.

The specimens had a cross section of 10x10mm and a length of 55mm, as shown in Figure 17. All test specimens will have a v-shaped notch in

the impact area, located at the centre of 55mm side. The samples were machined according to the British Standard BS-EN-10-045.

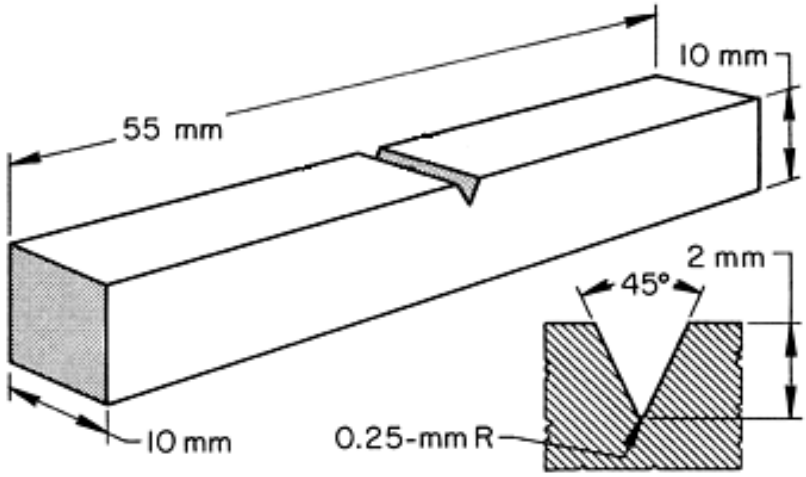

Figure 17. Measurements of the v- notch charpy specimen[17].

The test was performed on a Losenhausen machine, with 40kgm load. The temperature in the room was 21°C. The air-, bearing- and pointer friction was measured to 0.1kgm. The samples are cooled in a spirit solution for 10 minutes in order to obtain the desired temperature. The fracture surfaces of test specimens from the upper and the lower shelf of the charpy curve, from both the sandblasted and fractured chain, were examined and characterized in a Zeiss Ultra 55 scanning electron microscope (SEM).

The transition temperature between brittle and ductile fracture for the sandblasted steel was found in the project report from 2010[1], and can be seen in Figure 46 in the appendix.

3.3.4 Tensile test

It was necessary to conduct a tensile test for the fractured chain to find the materials ductility, yield strength and tensile strength. The yield strength of the material would be used to calculate the tensile stresses applied the specimens in the HISC rig. Also the strength of the material is needed to evaluate its susceptibility to HISC. The samples were taken from the unwelded bar in the long linked chain. The tensile curve for the sandblasted chain was found in the characterization project from the autumn 2010[1], and can be found in Figure 47 in the Appendix A. The test specimens were machined to the dimension showed in the Figure 18.

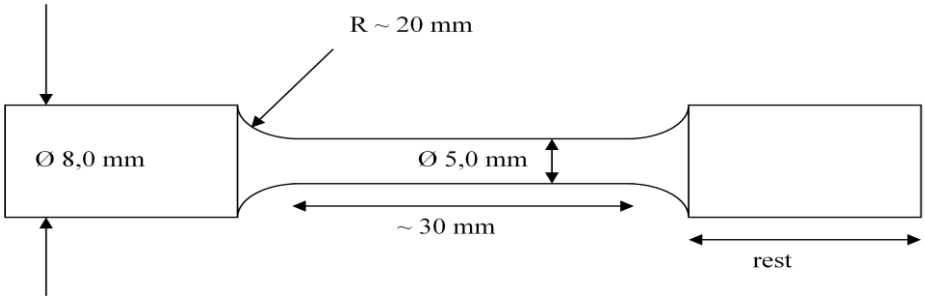

Figure 18. Design of the tensile test specimen.

3.3.5 Hydrogen charging of strain samples

One of the main purposes of this project was to evaluate the susceptibility of the chains to HISC. It was concluded in the report from 2010[1] that the sandblasted chain was susceptible to hydrogen embrittlement. It therefore anticipated that our specimens could fracture in a brittle manner due to HISC.

This was tested by making tensile specimens and subjecting them to tensile stresses in artificial seawater while they were exposed to hydrogen in a CorTest Proof rig. Both the fractured and the sandblasted chain were examined in the SEM. Fractured and un-fractured tensile specimens were evaluated in terms of their resistance to cracking during

hydrogen exposure and tension. Alternatively, the test could potentially reveal similarities between the two chain materials which could reveal weaknesses in the sandblasted chain, and simultaneously explain why the fractured chain had failed.

Making tensile specimens

For the constant load test a total of 25 tensile specimens were made from the sandblasted chain, plus 2 specimens from the fractured chain. All of the sandblasted chains were said to be from the same batch as the chains examined in the project from 2010 by Dahle [1]. The sandblasted chain rings were unused while the fractured chain had fractured in-service. No cracks were observed on the surface of any of the 4 chain rings.

The sketch in Figure 19 shows the measurements of the tensile specimen. The samples will be made with a length of 25.4 $\pm$ 0.2 mm on the middle with a diameter of Ø 3.81 $\pm$ 0.1mm. Then a quarter- hollow with a radius R of 15 mm was made out to the diameter which corresponds to the threads of UNF (unified fine) 7/16". The actual length of the tensile specimens was measured closer to roughly 85mm.

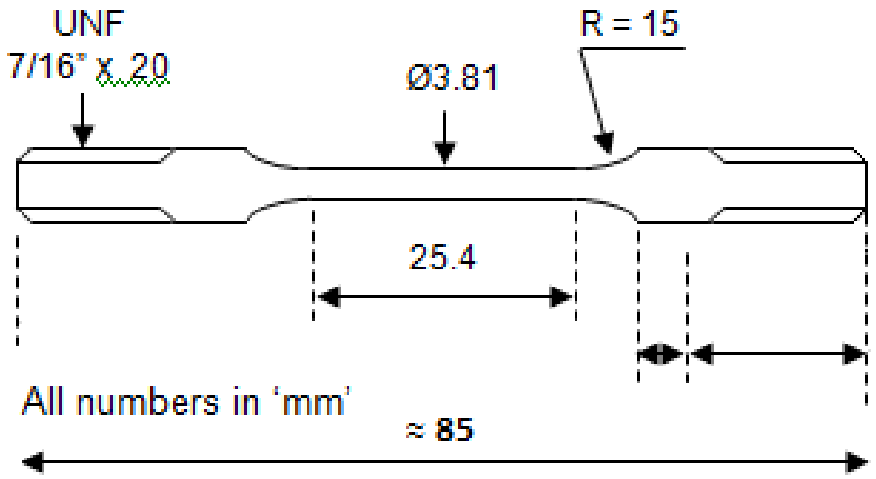

Figure 19. Dimensions of the threaded tensile specimen used in the CorTest.

When conducting the HISC tensile test it was desirable to evaluate how the sandblasted steel would react to hydrogen exposure if the HDG coating was damaged. This situation is highly relevant for what chains are exposed to in-service were friction between chain rings wear down the coating, exposing steel to the environment. A total of eight of the sandblasted tensile specimens were re-galvanized. The design of the new galvanization layer can be seen in the Figure 20. Figure 20 shows a specimen recoated with zinc. The threads have not been coated because they have to be threaded into the test rig. At the middle of the specimen a belt with an approximate width of 10mm was left ungalvanized to simulate an injury in the coating. The area selected not to be HDG was coved by a masking tape when dipped into the zinc bath. During exposure in the HISC rig the HDG sample will absorb hydrogen differently to the sample without zinc.

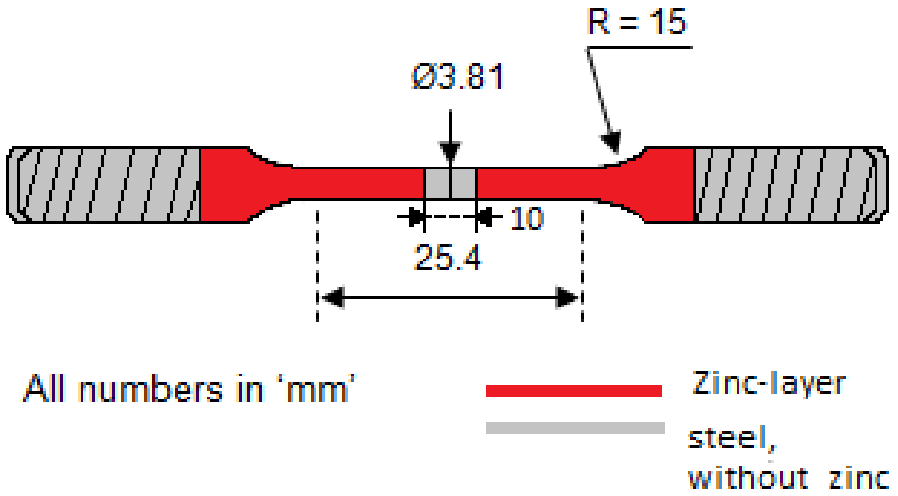

Figure 20. Design of the re-galvanized threaded tensile specimen.

When re-galvanized, the tensile specimens were first cleaned by acid pickling for 20 minutes at Ferrozink AS, in Trondheim. The specimens were then HDG for 2 minutes at roughly 450°C. The thickness of the HDG layer was not measured.

Sample preparation

Before precharging the tensile specimens they needed to be properly cleaned. First they were cleaned with acetone and placed in an ultrasound bath for 20 minutes. The specimens were then rinsed with ethanol. A platinum wire was wrapped around the specimens to conduct the current from the potensiostat. When charging the tensile specimens with hydrogen, it is desirable to avoid exposure for the threads. If the threads got embrittled by the hydrogen they would become a weak point and fracture prematurely. Therefore, the threads on both ends were covered by a heat-shrink sleeve. The bottom end, without a platinum wire was sealed with a rubber cork. The platinum wire, on the top half, was allowed to protrude out the end to connect the sample to the "working" terminal on the potensiostat.

Hydrogen charging procedure

Prior to the HISC tensile tests the test specimens was charged with hydrogen to ensure a presence of hydrogen in the specimens. This was done in a 3L jar with 3.5% NaCl solution. The setup of the precharging equipment can be seen in Figure 21. The potentiostat was set to deliver a potential of -1050mV vs. Ag/AgCl to the ungalvanized tensile specimens, and the solution was held at a room temperature (21°C).

A glass tube wrapped with platinum wire was placed though the lid of the jar and was connected to the "counter" terminal of the potensiostat. The bottom of the tube was plugged with a cotton stopper to allow electrical conductivity but no electrolyte flow. The temperature regulating thermometer probe for the heating element was also placed though a hole in the lid. Other holes in the lid were sealed as tightly as possible to minimize electrolyte loss due to evaporation.

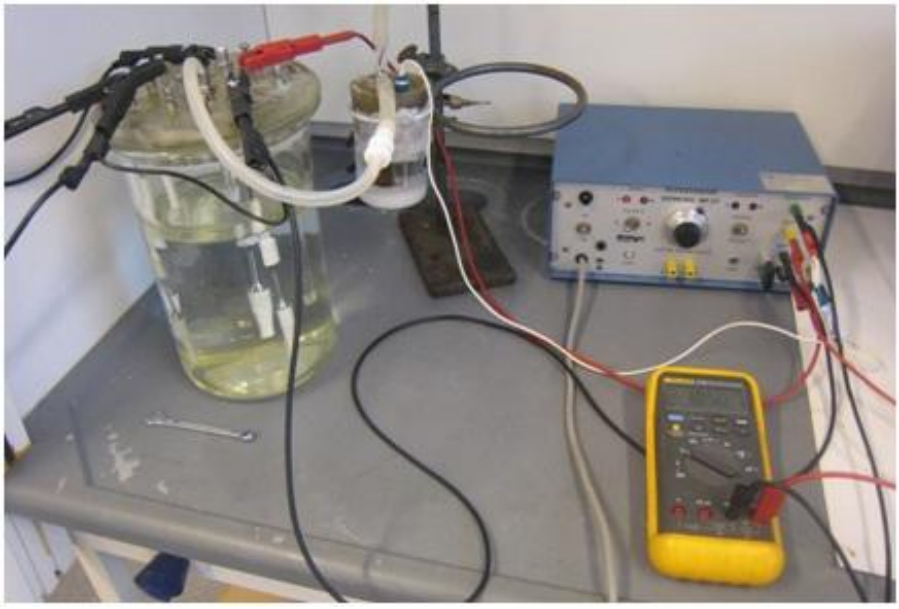

Figure 21. Test setup for the precharging of test specimens for use in the HISC rig.

Some tensile specimens were re-galvanized, according to the design of Figure 20. One reason for selecting a damaged, galvanized test specimen was to attempt to recreate a situation which would be realistic for anchor chains while they were in use. The results of the ungalvanized specimens would be compared to the results of the HDG specimens to see if there were any differences in their resistance to HISC.

The re-galvanizes specimens were also charged with hydrogen. This was done by exposing the specimens in a 3L jar with 3.5% NaCl heated to 40°C for 10 days. The specimens would corrode freely without an external potential, so that the "damaged" area would be protected by the zinc as a CP. With this design the zinc could potentially generate hydrogen on the steel metal surface. The increased temperature increases the speed of which hydrogen diffuse into the lattice structure of the metal. A summary of the hydrogen loading parameters can be found in Table3[18].

Table 3. Hydrogen loading parameters according to the type of tensile specimen.

Sample type	# Samples	Temp [°C]	Potential [mV vs. Ag/AgCl]	Charging [days]
Unprotected, fractured tensile specimen	2	21	-1050	10
Unprotected, sandblasted tensile specimen	8	21	-1050	10
HDG, sandblasted tensile specimen	8	40	Free corrosion	10

Unprotected tensile specimens, set to corrode freely in the HISC test, were not precharged with hydrogen. The specimens were however cleaned in acetone before they were put into the test rig.

Removal of test specimens

When the hydrogen charging period was complete and the specimens were ready to be removed from the loading cell, the specimens were prepared for immersion into the CorTest Proof ring unit. The jar lid was lifted off and the specimens were disconnected from the rig, and the heat-shrink coating was cut off the tensile specimens. The specimens were then mounted into the environment container in the HISC rig. The environment container was then filled with 3.5% NaCl, and a potential of -1050mV vs. Ag/AgCl is again connected to the relevant test specimens

3.3.6 Constant load test

The submerged tensile test was conducted on CorTest Proof Rings according to NACE TM0177[19]. A picture of the test rig can be seen in Figure 22. The CorTest Proof ring unit is designed to facilitate testing and material evaluation in many in environments with a short setup time and with mechanical loading equipment.

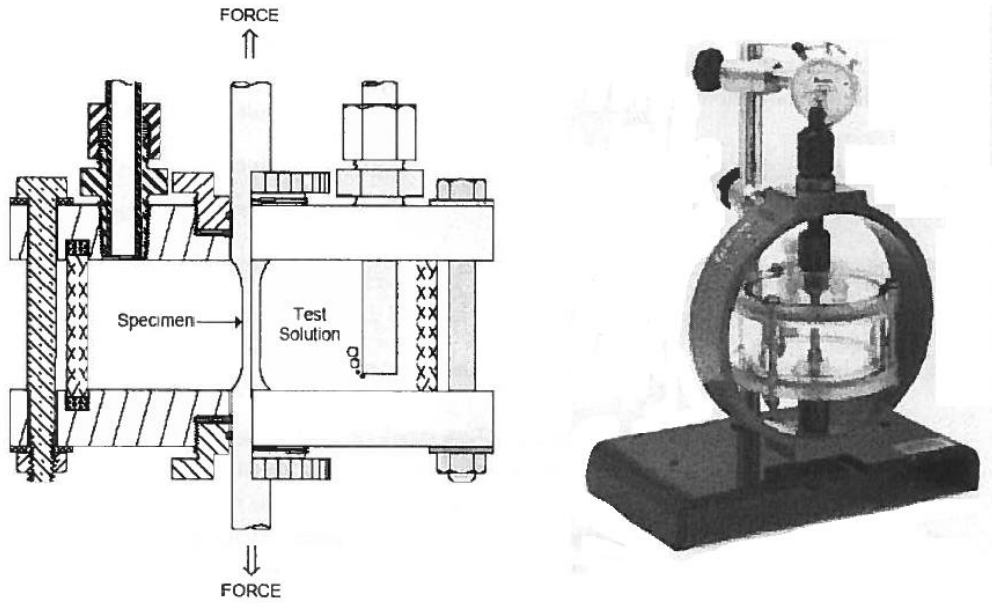

Figure 22. Description of test unit (left) and a picture of the CorTest Proof ring set up (right)[20].

Assembly

The working procedure for the constant load testing is described in Sintefs internal document number KS-802829-WP-005[20]. The procedure is based on the standard NACE TM 0177-96[19] about laboratory testing for resistance to sulfide stress cracking in hydrogen sulfide environments.

The assembly of the CorTest Proof ring unit was started by inserting the tensile specimen into the environment container with the ends of the specimen protruding out of its top and bottom. The container was sealed by placing rubber O-rings around each shoulder of the tensile specimen. The o-ring seals were activated by screwing acrylic end plates onto the containers top and bottom. In the next step one attached the upper and lower specimen grip to the tensile specimens. The specimen grips were used to attach the container into the CorTest Proof ring. When attached, the loading rod was screwed into the end grip. The bearing and loading

nut was then placed on the adjusting screws. Then, one could hand tighten the assembly to the desired stress level, by using the loading nut, and measure the displacement of the proof ring. The finished assembly can be seen in Figure 23. For a more detailed description of the working procedure see Sintefs internal document for "*General description of the working procedure for – Constant load testing*[20]".

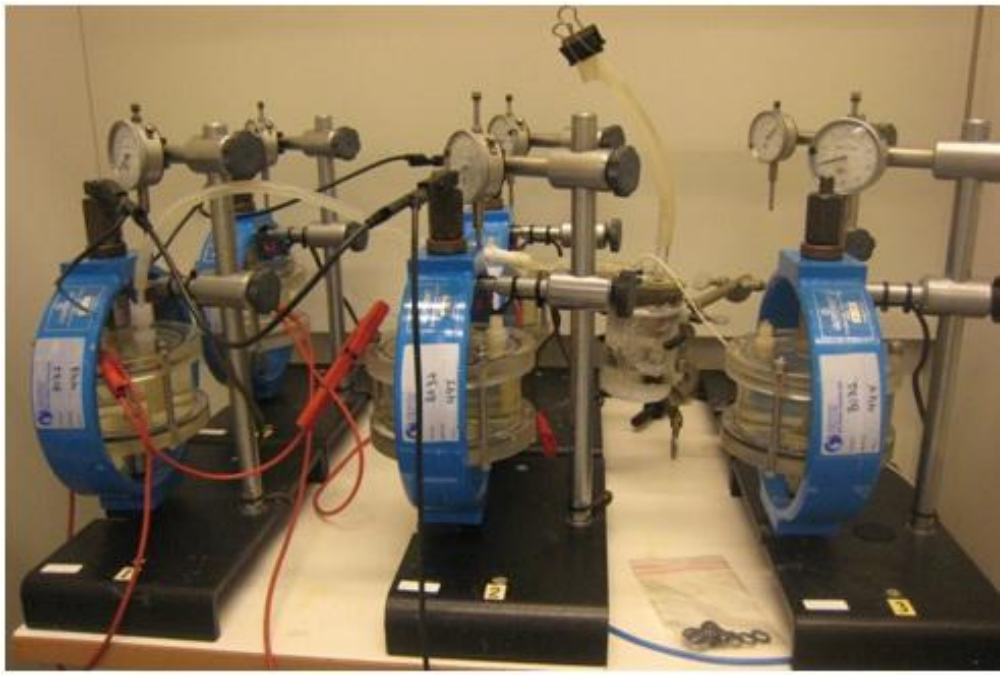

Figure 23. Picture of the HISC constant load test set-up.

In the test setup in Figure 23 several proof rings are coupled to a potensiostat. The potensiostat supplies a potential of -1050mV vs. Ag/AgCl which protects the steel specimens from corroding. The coupling between the potensiostat, proof rings (test specimens) and the Ag/AgCl reference cell is depicted in the schematic in Figure 24.

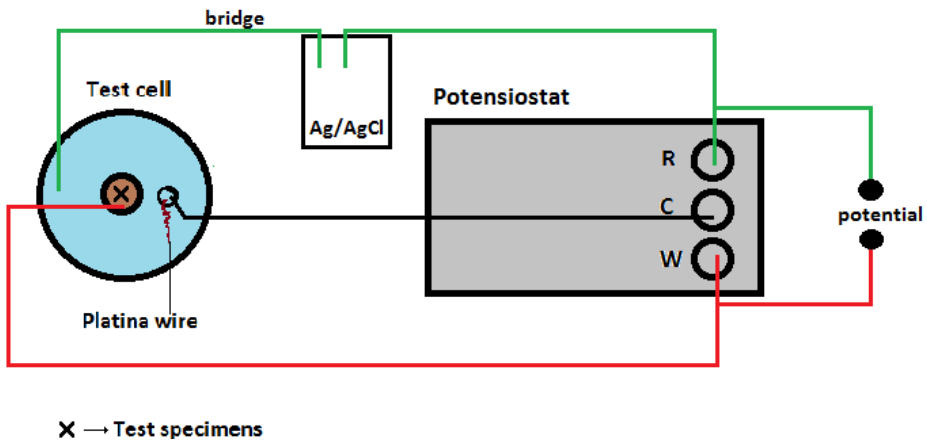

Figure 24. Potential setup diagram for the HISC rig system.

Test procedure

A plan for the HISC test was established and the test program is presented in the matrix in Table 4. Initially, it was decided to find the fracture limit of the steels while they were exposed to hydrogen in artificial seawater at their respective corrosion conditions. The test was started by applying a force equivalent to 90% of yield strength, $\sigma_{Y,S}$, for the sandblasted chains. The two fractured tensile specimens was also initially pulled by a force of 90% of the its yield strength, $\sigma_{Y,F}$. Consequently, the force applied to the fractured and sandblasted test specimens would increase by +2% of $\sigma_{Y,F}$ or $\sigma_{Y,S}$ every second day until the specimens fractured.

The further progress of the test program would be determined by the outcome of the verification phase 2. In the verification phase 2 the specimens would be stretched to a tension of 95% their respective tensile strength for 14 days. If the specimens fractured during loading, the test would imply that they had become brittle and that they did not resist the load.

If a specimen fractured while loaded to 95% of its tensile strength for 14 days, the next step would then be to apply a tension equivalent to 90% of their respective tensile strength. The reason for this approach is to

attempt to find the limit between the materials brittle and non-brittle behavior, which would mean finding a safety limit. However, if the specimens do not fracture at the load of 95% of their tensile strength, the next step will be to increase the load to 100% of their tensile strength (verification 3.B phase). If specimens did not fracture but developed microcracks on the gauge section, it would indicate that HISC or pitting corrosion could be initiated. Microcracks are undesirable because they indicate that the material is not fully resistant to HISC.

The actual test plan can be found in Table 16 and Table 17 in Appendix B – Experimental results.

Table 4. Test program and sample selection for HISC test.

TEST TYPE	SB	SB + HDG	F	Comments	#Sample
Screening phase 1 *90% of $\sigma_{Y,S}$ + 2% increase/2.day* • Charged at -1050mV$_{Ag/AgCl}$ • Free exposure	2 1	 1[1)]	2	This is to find the fracture limit σ for samples	6
Verification phase2: *95% of $\sigma_{F,S}$ for 14 days* • Charged at -1050mV$_{Ag/AgCl}$ • Free exposure	2 1	 2[1)]		The purpose is to examine if the specimens will fracture under this load. The sample surfaces are examined for microcracks.	5
Verification phase 3.A: *100% of $\sigma_{F,S}$ for 14 days* • Charged at -1050mV$_{Ag/AgCl}$ • Free exposure	2 1	 2[1)]		Only if loading to 95% of σ_F **does not give** cracking/ -fracture in the samples	5
Verification phase 3.B: *90% of $\sigma_{F,S}$ for 14 days* • Charged at -1050mV$_{Ag/AgCl}$ • Free exposure	2 1	 2[1)]		Only if loading to 95% of σ_F **gives** cracks/fracture in the samples	5
# Samples	9 (12)	5 (7)	2		**16 (20)**

1) Sandblasted samples are exposed freely in 40^{0}C 3.5% NaCl solution for 10 days

Hydrogen saturated specimens are loaded according to the procedure described in chapter 3.3.5. In the HISC test the specimens were subjected to three different corrosion potentials. They specimens would either be;

- protected by applying a protection potential of -1050mV vs. Ag/AgCl, and thereby making the steel immune to corrosion. These specimens were charged at the same potential
- set to corrode freely, without corrosion protection
- or protected by applying a zinc coating which works as a CP. These specimens were charged at corroding freely in a seawater bath at 40°C.

The abbreviations in Table 4 stand for:
F is short for fractured chain. SB means sandblasted chain. $\sigma_{F,S}$ is the symbol for the sandblasted steels tensile strength. The $\sigma_{Y,S}$ stands for the sandblasted steels yield strength. The sandblasted chain has a known fracture limit of $\sigma_{F,S}$ = 1070MPa and a $\sigma_{Y,S}$ = 1030MPa, while the values for the fractured chain needed to be established.

To keep track of the specimens and to separate them from each other they were given appropriate names. As an example sample *CorTest24.s(galv)* is mentioned. Here, *CorTest* means it has been tested in the CorTest Proof ring. The second part of the name is the number *24*, indicating the specimen number. Each number represents a different chain link. The third part is the lettes *s* or f. That letter means that the specimen was either taken from the sandblasted chain or the fractured chain. The forth segment of the name is placed in brackets. In the example, the bracket contains the word *galv* which means the specimen was HDG. Alternatively, the brackets can contain the word *free*, revealing that the specimens have corroded freely in the CorTest Proof ring during its test period with any corrosion protection. No brackets

indicate that the specimens were supplied with a potential of -1050mV vs. Ag/AgCl during its precharging and its loading period in the HISC test.

Each of the five CorTest Proof rings (rig1, rig2, rig3, rig4 and rig5) which were used in this experiment has their own default distance (h_0) between the top and bottom of the ring when they are unloaded. How this is measured can be seen in Figure 25. All displacements are measured against this default position. The default distances are a presented in Table 5.

Table 5. Default height of the five CorTest Proof rings used during this experiment.

Rig #	Cell #	Default height h_0 [mm]
1	2622	219.21
2	2623	219.09
3	2628	219.22
4	2629	219.21
5	2630	219.21

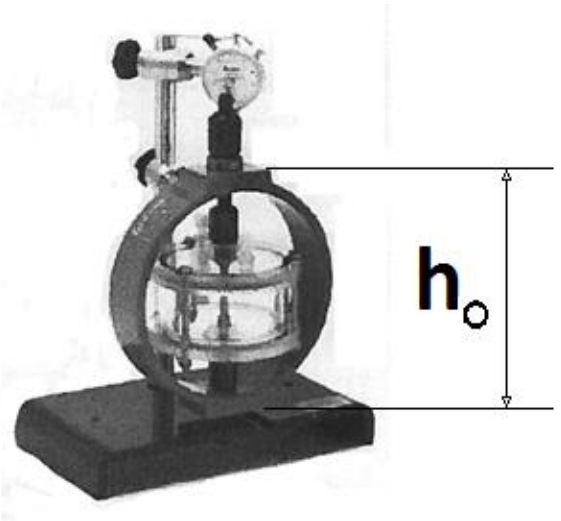

Figure 25. How to measure the default height of the CorTest Proof rings and the displacement from it during loading.

3.3.7 SEM fractography

To evaluate if our samples were subjected to enough hydrogen during preloading and the tensile testing to cause a brittle fracture, it was decided to characterize the specimens fracture surface in a SEM. If tensile specimens subjected to constant load for 14 days did not fracture during the test, the specimen surface would be examined for microcracks. If microcracks are observed it means that HISC may be initiated, but that the cracks have stopped growing.

The fractographic examinations were performed on a Zeiss Ultra 55 SEM. Before putting specimens into the SEM vacuum chamber they were submerged in acetone and put in an ultrasound bath for 15minutes. Afterwards they were rinsed in ethanol an air dried.

4 Results

4.1 Characterization of fractured anchor chain

4.1.1 Microstructure

The image of the microstructure in Figure 26, from the fractured anchor chain, resembles a tempered martensite structure. Here ferrite and carbides are barely resolved. Characteristic for martensite structure is the lath or needle shapes on the surface. The image was taken from the center of the hardness sample 4.T.a.

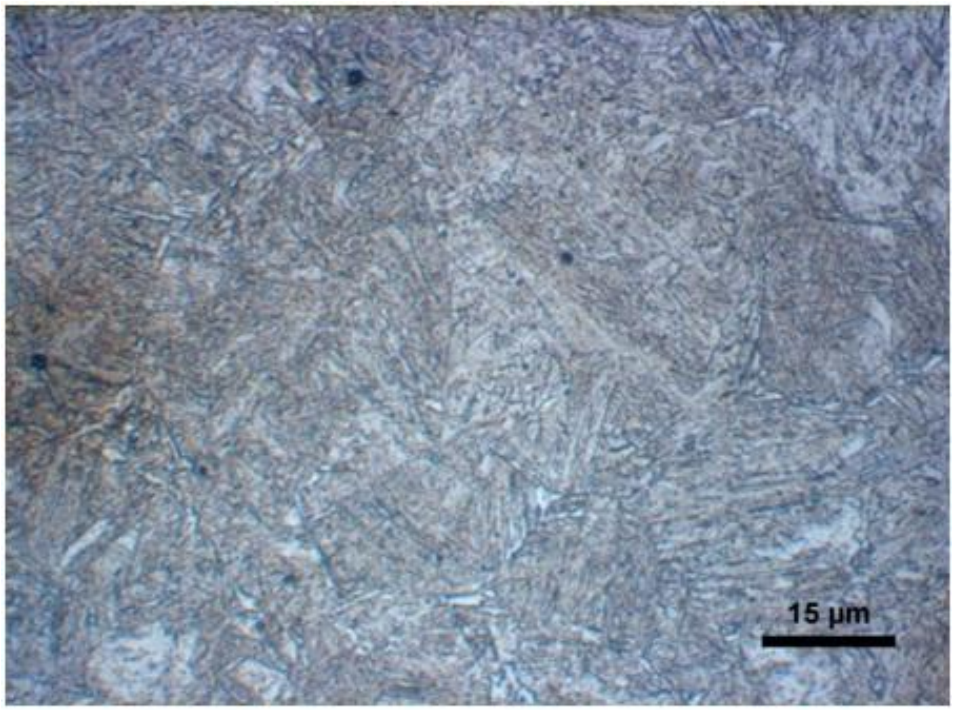

Figure 26. Microstructure of the fractured anchor chain. Magnification is given by the scale bar.

4.1.2 Hardness

The average hardness of fractured anchor chain was 381 ± 8 HV with 10kp load. This corresponds to an average indentation diameter of 221µm. The hardness of the sandblasted chain was previously found to be 367 ± 12 HV [1].

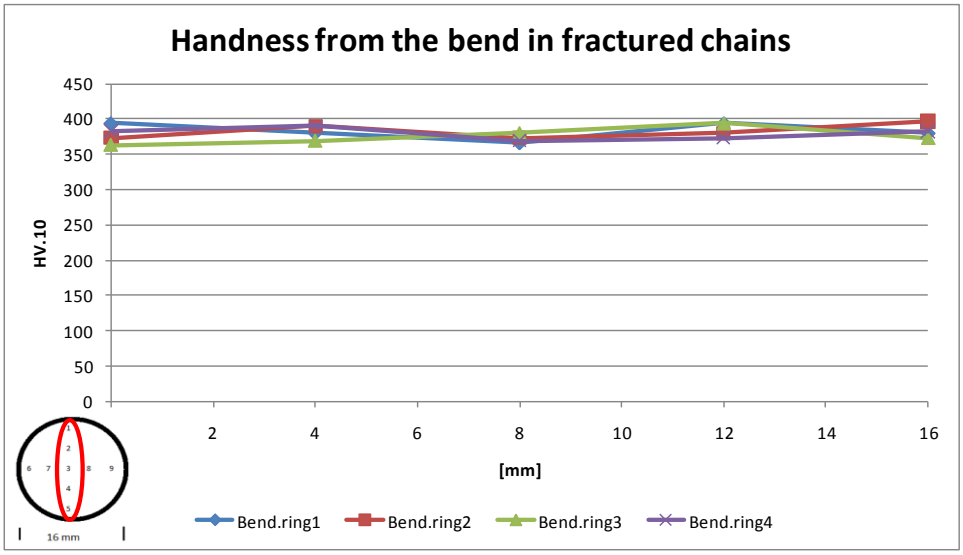

Figure 27. Longitudinal hardness profile from the bend of the fractured anchor chain.

The hardness profile for position 1 to 5, for the four examined chain rings, in Figure 27 above seems to have no degree of hardness variations. The material is considered to have good homogeneity. Compared to the sandblasted chain, the homogeneity is better. The hardness measurements also generated a transverse hardness profile for the bend, which can be seen in Figure 48 in Appendix B – Experimental results.

4.1.3 Charpy

Fractured chain

The impact energies for the fractured chain steel over temperature are given in Figure 28. The transition temperature between brittle and ductile fracture for the fractured chain was not found for the test temperatures used in the experiment.

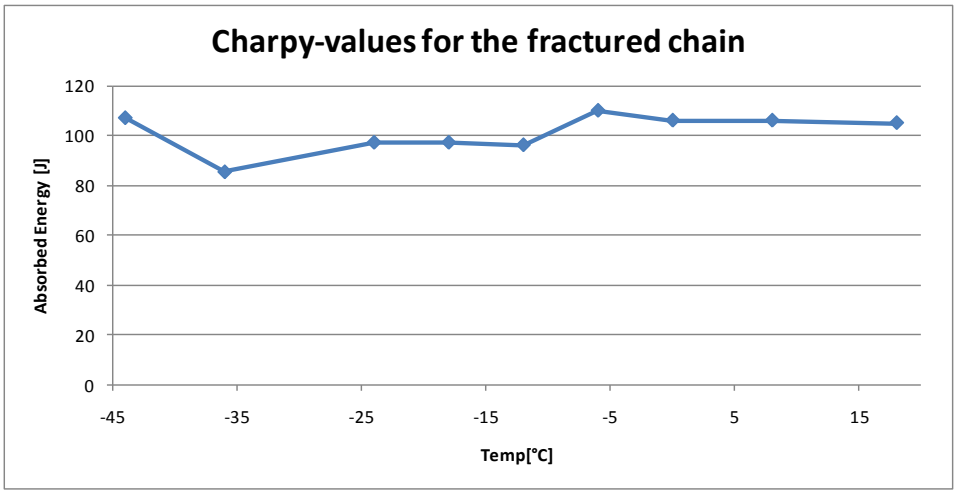

Figure 28. Charpy values for the fractured chain steel.

The fracture surface of charpy specimen 1 and 9, tested at 18°C and -44°C respectively, were examined in an SEM and characterized.

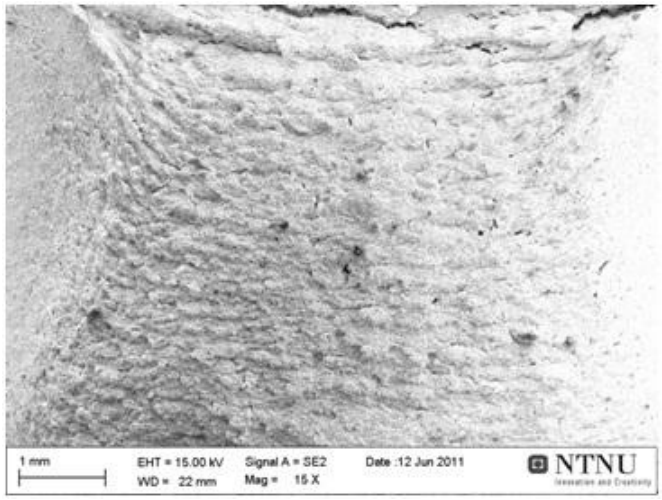

Figure 29. Fracture surface of charpy specimen 1 at 15x magnification.

Figure 29 show the fractography of charpy specimen 1 at 500x magnification. Figure 30 shows the same sample at a magnification of 1000x.

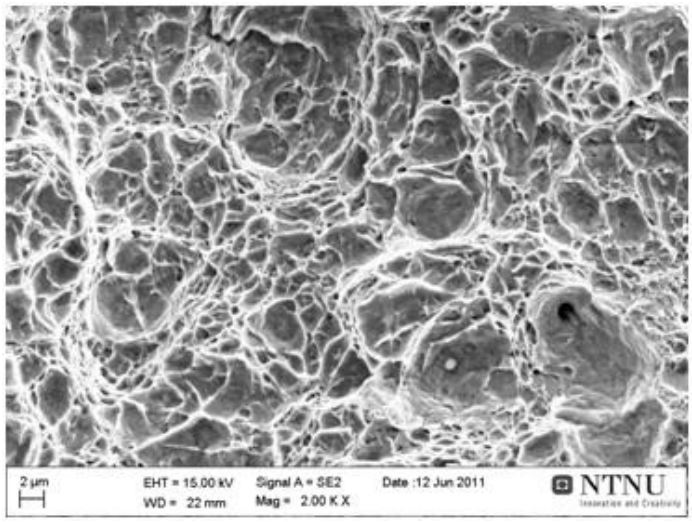

Figure 30. Fracture surface of charpy specimen 1 at 2000x magnification.

The fracture surface is marked with dimples which are a sign of a ductile fracture. Specimen 9, tested at -44°C, was also examined. Figure 31 and Figure 32 below shows the topography of the sample at 500x and 1000x magnification respectively.

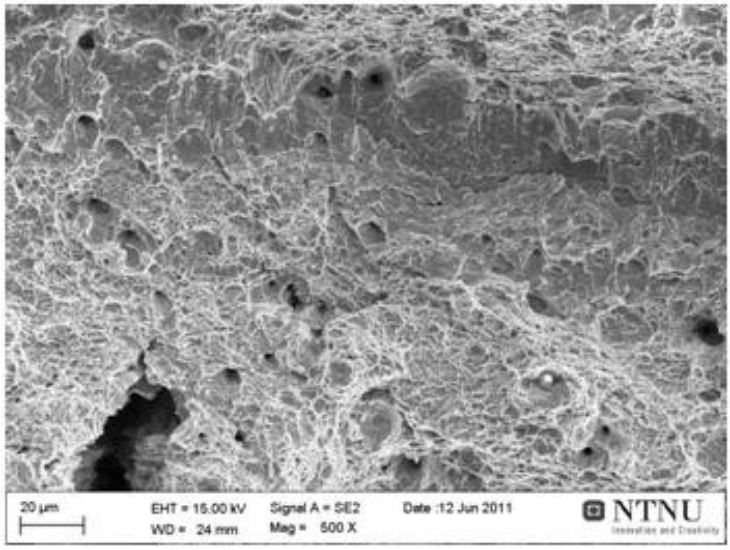

Figure 31. Fracture surface of charpy specimen 9 at 500x magnification.

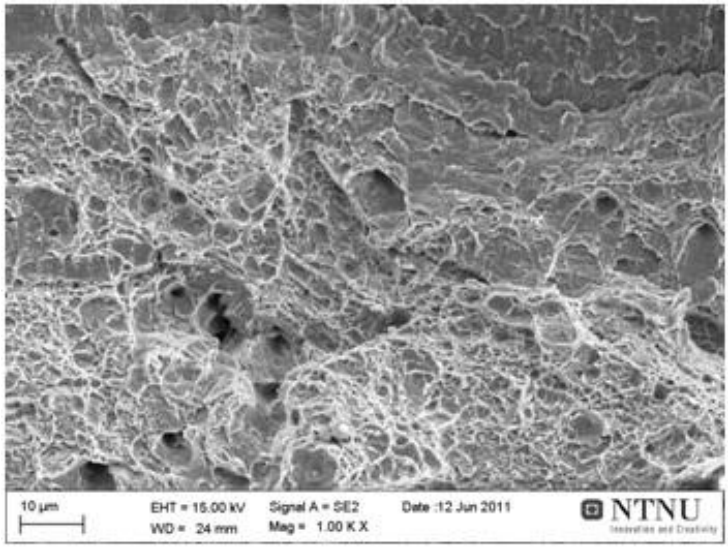

Figure 32. Fracture surface of charpy specimen 9 at 1000x magnification.

In Figure 32 a mixture of dimples and cleavage facets can be observed, indicating a quasi-cleavage fracture. The impact value of 80J suggests the specimen is not purely brittle.

4.1.4 Tensile test

The yield strength of the fractured chain material was read off the curve in Figure 33 to be 890MPa, while the tensile strength was 980MPa. The elongation to fracture of the materials was nearly 16% (15.9%). The tensile curve for the sandblasted chain material is presented in Figure 47 in Appendix A – Previous work.

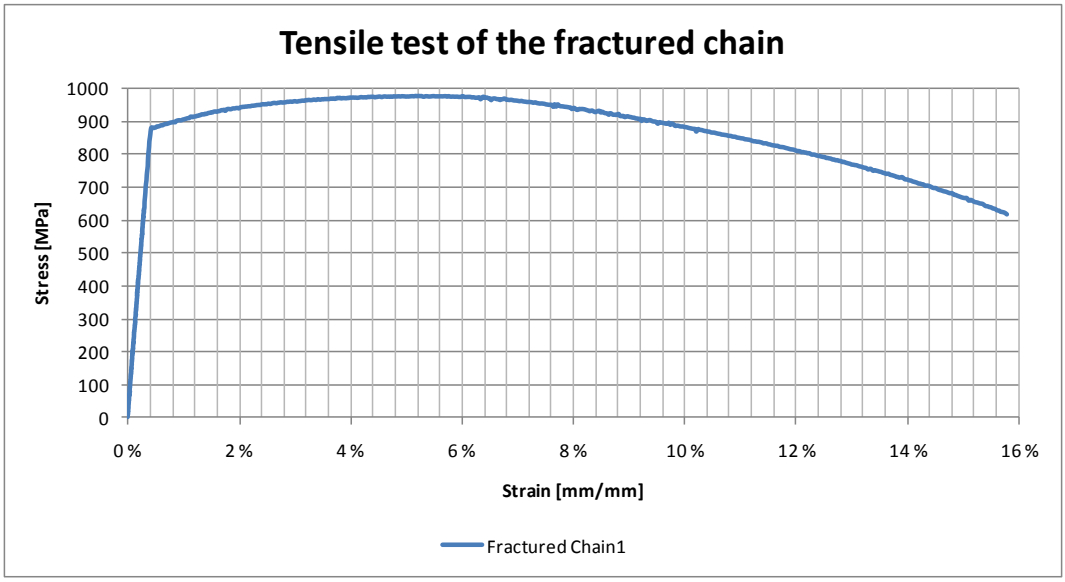

Figure 33. Stress- strain curve of the fractured chain steel.

According to the conversion *table B.2 – conversion of hardness-to-hardness and hardness-to-tensile-strength values for quenching and tempering steels in the quenched tempered condition* in ISO 18265 a hardness of 381HV.10 or 367HV.10 correspond to a tensile strength of 1192MPa and 1149,7MPa respectively. The values were found by interpolating in the table.

4.2 HISC test

4.2.1 Results

The results of the HISC test are presented in Table 6, 7 and 8 and are divided into their three phases as proposed in Table 4. The tables contain information on which initial and final load each of the specimens were subjected to during their test period measured towards the materials yield strength. The yield strength of the sandblasted and the fractured chain is 1030MPa and 890MPa respectively. The 3.5% NaCl solution held a temperature of 21°C and had a pH value of 6.5 at the start of the experiment.

At a pH of 6.5 the hydrogen reduction reaction (equation 1, page 8) can occur below the potential E_0 = -384mV, found from equation 6. The calculation can be seen in Attachment B.14 in Appendix B – Experimental results.

Because of time shortage, only a selection of specimens was examined in the SEM. Specimens marked with a question mark (?) in the columns were not examined in the SEM for microcracks. Fractured specimens automatically qualify for cracking. Information on the exposure time for each specimen in the HISC rig, until test stop or fracture, is also included in the tables. Some specimens fractured during the test, while others did not. Selected specimens which did not fracture were examined for surface cracks.

Screening phase 1

The first tensile specimens were a part of the screening phase. In Table 6 one can see at which load these specimens fractured. In the screening phase specimens were deliberately pulled until fracture, so that the fracture load of the specimens could be found at their respective corrosion potentials. Detailed information about the gripping tension calculations and loading sequences of each specimen can be found in Attachment B.4 to B.11 in Appendix B – Experimental results.

For the sandblasted specimens, it can be seen from Table 6 that the unprotected specimen fractured at a load close to 1050MPa. The specimens polarized to -1050mV vs. Ag/AgCl fractured at a slightly higher load, close to 1070MPa. HDG specimens took the highest load before fracturing. Here, the HDG specimens fractured at a load equal to 1130MPa.

The fractured specimens, *CorTest1.f* and *CorTest2.f*, failed at a load equal to their tensile strength (980 MPa).

Table 6. Test results from the screening phase of the HISC tensile test.

Sample	Initial Load (MPa)	Initial load- % if yield strength	Final load- % of yield strength	Exposure Time (h)	Fracture	Observed Cracking
CorTest1.s	909	88 %	~ 106 %	483.2	Yes	Yes
CorTest2.s	909	88 %	~ 104 %	434.3	Yes	Yes
CorTest3.s(free)	909	88 %	102 %	385.2	Yes	Yes
CorTest25.s(galv)	927	90 %	110 %	603.7	Yes	Yes
CorTest1.f	801	90 %	110 %	481.6	Yes	Yes
CorTest2.f	801	90 %	110 %	481.6	Yes	Yes

The HDG specimens have their own protection potential. The protection potential on the HDG steel, of tensile specimen *hisc.25.s.(galv)*, was measured to -904mV vs. Ag/AgCl against saturated calomel. For the specimens without CP or HDG layer the corrosion potential was anticipated to be in the range of -550 to -600mV vs. Ag/AgCl (not measured).

Verification phase 2

In phase 2 each specimen was set to a load of 95% of the materials tensile strength. By mistake specimen *CorTest5.s* and *CorTest7.s(free)* was loaded to 95% of the materials yield strength. As seen from the

Table 7 microcracks were discovered for the unprotected specimens and the specimens polarized to -1050mV vs. Ag/AgCl , but not for HDG specimens.

Table 7. Test results from verification phase 2 of the HISC tensile test.

Sample	Initial Load (MPa)	Initial load- % if yield strength	Final load- % of yield strength	Exposure Time (h)	Fracture	Observed Cracking
CorTest5.s	979	95 %	95 %	363.9	No	?
CorTest6.s	1017	~ 100 %	~ 100 %	363.2	No	Yes
CorTest7.s(free)	979	95 %	95 %	361.0	No	Yes
CorTest13.s(galv)	1017	~ 99 %	~ 99 %	330.5	No	?
CorTest14.s(galv)	1017	~ 99 %	~ 99 %	330.3	No	no

Verification phase 3.B

In phase 3.B each specimen was set to a load of 100% of the materials tensile strength. By mistake specimen *CorTest10.s*, *CorTest11.s,* and *CorTest12.s(free)* was removed from the test rig after 8 days instead of 14 days. This explains why the exposure times of the specimens were below 200 hours. They were therefore replaced by specimen *CorTest15.s*, *CorTest16.s* and *CorTest17.s(free)* in order to ensure reliable test results.

As seen from the Table 8 microcracks were discovered on the unprotected specimens and the specimens polarized to -1050mV vs.Ag/AgCl. HDG specimen *CorTest18.s(galv)* was not examined for microcracks, but fractured prematurely and cracking is therefore observed

Table 8. Test results from verification phase 3.B of the HISC tensile test.

Sample	Initial Load (MPa)	Initial load- % if yield strength	Final load- % of yield strength	Exposure Time (h)	Fracture	Observed Cracking
CorTest10.s	1070	~ 104 %	~ 104 %	195.2	No	?
CorTest11.s	1070	~ 104 %	~ 104 %	194.6	No	?
CorTest12.s(free)	1070	~ 104 %	~ 104 %	195.6	No	No
CorTest15.s	1070	~ 104 %	~ 104 %	364.0	Yes	Yes
CorTest16.s	1070	~ 104 %	~ 104 %	363.5	No	Yes
CorTest17.s(free)	1070	~ 104 %	~ 104 %	406,9	Yes	Yes
CorTest18.s(galv)	1070	~ 104 %	~ 104 %	70.7	Yes	Yes
CorTest24.s(galv)	1070	~ 104 %	~ 104 %	336.0	No	No

4.2.2 Fracture surfaces

The tensile specimens which fractured during the HISC test at their respective load are listed in Table 9. SEM pictures from the screening phase 1 are included in the report, while SEM pictures of the fractured specimens from verification phase 3.B are put in Attachment B.12 in Appendix B – Experimental results.

Table 9. List of tensile specimens which fractured during the HISC test.

Specimen	Fractured	Examined in the SEM
Screening phase 1:		
CorTest1.s	Yes	No
CorTest2.s	Yes	Yes
CorTest3.s(free)	Yes	Yes
CorTest25.s(galv)	Yes	Yes
CorTest1.f	Yes	No
CorTest2.f	Yes	Yes
Verification phase 3.B:		
CorTest15.s	Yes	Yes
CorTest17.s(free)	Yes	Yes
CorTest18.s(galv)	Yes	Yes

Specimen *CorTest15.ss* and *CorTest.s.18.galv* were deliberately pulled to fracture after the 14 day period of constant loading by increasing the load by 5% of the materials tensile strength.

Fractured chain

The following pictures are taken of sample *CorTest2.f*. Figure 34a shows a classic ductile fracture surface. Three distinct zones can be observed. The outer zone is the shear lip, while the middle zone is called the radial zone and the inner zone is called the fibrous zone. The dimples in Figure 34b verify this observation. There was unfortunately no time to take SEM pictures of *CorTest1.f* due to lack of time.

Specimen *CorTest2.f*

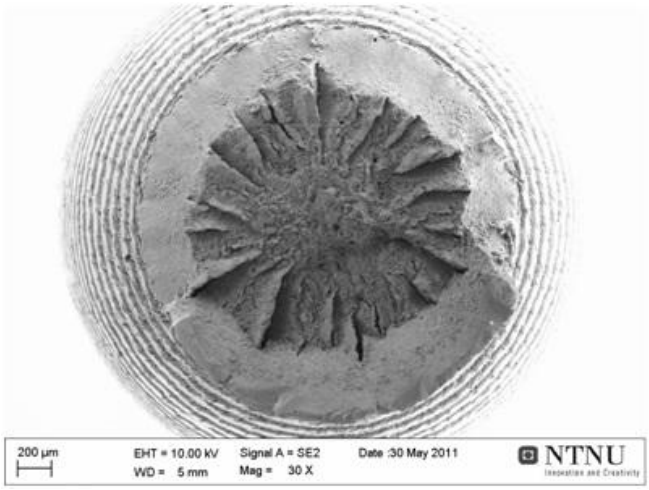

a)

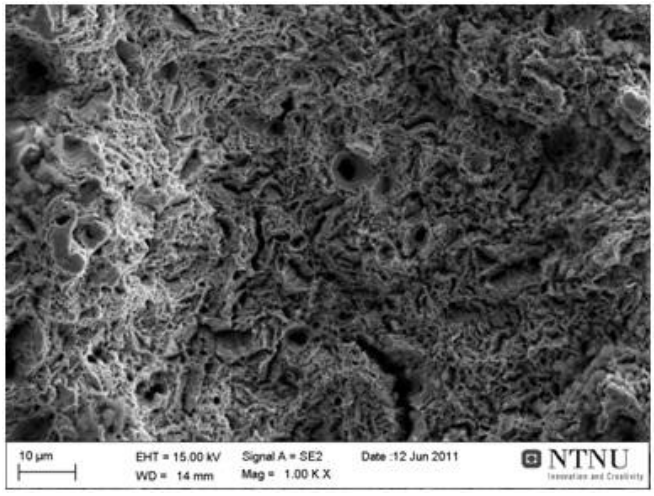

b)

Figure 34. a) Macroscopic view of the tensile specimen *CorTest2.f* of the fractured chain at 30x. b) Fractographic photo of the center of sample *CorTest2.f* at 1000x.

Sandblasted chain

SEM pictures of specimen *CorTest2.s*, *CorTest3.s(free)* and *CorTest25.s(galv)* are presented in the report. The specimens from verification phase 3.B are presented in Appendix B – Attachment B.12. The specimens from the screening phase 1 have dimples in their fracture surfaces indicating ductile overload fractures.

Specimen *CorTest2.s*

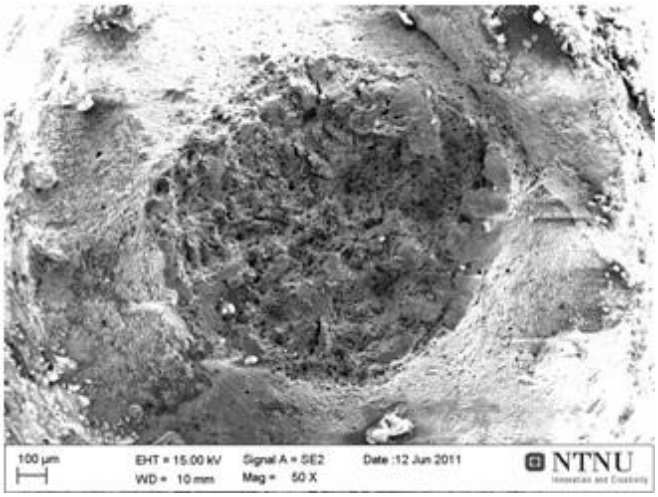

a)

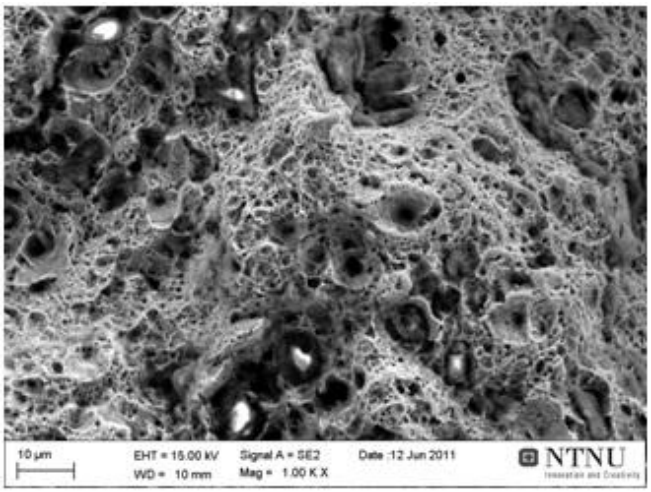

b)

Figure 35. a) Fractographic overview of the sandblasted tensile specimen *CorTest2.s* at 50x. b) Fracture surface of tensile specimen *CorTest2.s* at 1000x.

Specimen *CorTest3.s(free)*

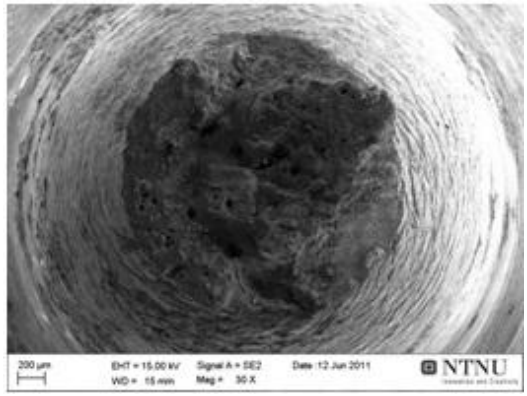

a)

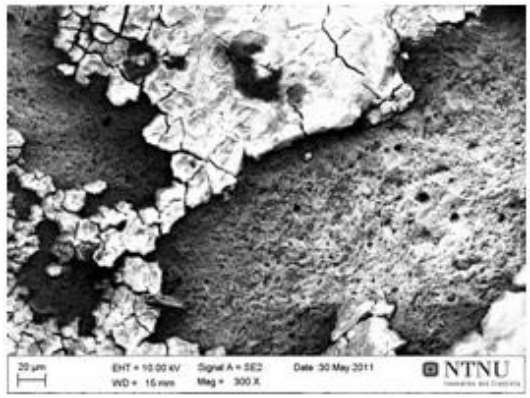

b)

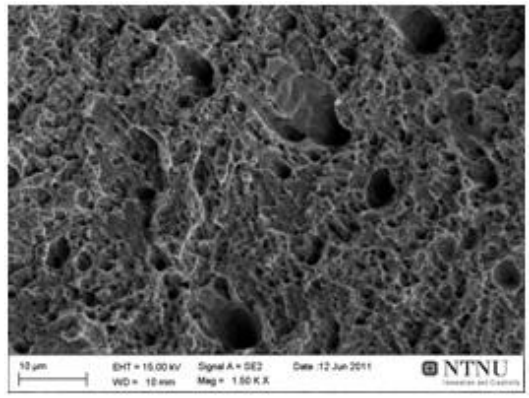

c)

Figure 36. a) Fractographic overview of the sandblasted tensile specimen *CorTest3.s(free)* at 30x. b) Fracture surface of tensile specimen *CorTest3.s(free)* at 300x. Corrosion product on the sample can be seen. c) Sample *CorTest3.s(free)* magnified at 1500x showing dimples, indicating a ductile fracture.

Specimen *CorTest25.s(galv)*

Figure 37 shows a typical cup shape, as discussed in the theory, with dimples covering the fracture surface. The HDG specimen *CorTest25.s(galv)* appears to be ductile.

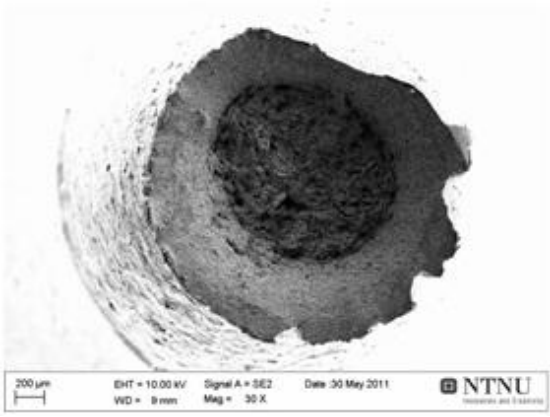

a) Macro photo of *CorTest25.s(galv)* at 30x.

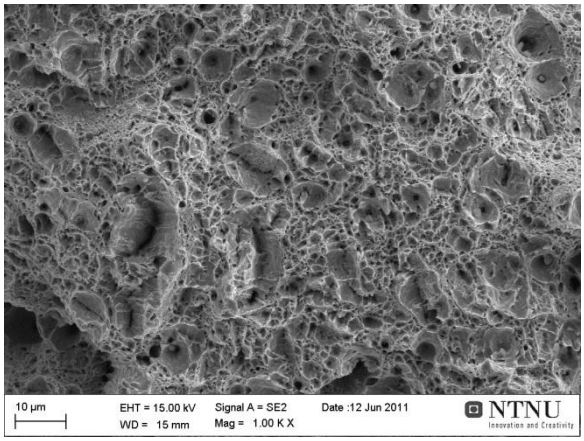

b) Center of specimen *CorTest25.s(galv)* at 1000x

Figure 37. a) Fractographic overview of the sandblasted tensile specimen *CorTest25.s(galv)* at 30x. b) Sample *CorTest25.s(galv)* magnified at 1000x showing dimples, indicating a ductile fracture.

Ductility

The reduction of cross section areal is an indication of the ductility of the specimen. The cross section of the fractured specimen was therefore measured with a mm-slide caliper at the point of fracture. A large degree of area loss would indicate that the ductility of the specimens were intact despite the exposure to hydrogen.

The area reduction was calculated by the formula[13];

$$\% \text{ reduction in area} = \frac{A_0 + A_f}{A_0} \times 100 \quad (8)$$

Here, A_0 is the original cross-section area and A_f is the final cross-section area at the fracture surface. The results can be seen in Table 10. The final cross section was measured at the tip of specimen. Three measurements were made for each specimen. The average of the three measurements was used as A_f.

Table 10. Results from the measurements of the reduction in cross section area to fracture.

Sample	Initial cross section [mm]	Final cross section [mm]	Area reduction [%]
CorTest.s.1	3,70	2,40	35,14
CorTest.s.2	3,71	2,56	31,00
CorTest.s.3.fritt	3,87	2,25	41,86
CorTest.s.25.galv	3,67	2,27	38,15
CorTest.s.15	3,67	2,26	38,42
CorTest.s.17.fritt	3,56	2,06	43,87
CorTest.s.18.galv	3,88	2,88	34,72
CorTest.f.1	3,75	2,77	35,38
CorTest.f.2	3,73	2,41	35,39

4.2.3 Search for surface microcracks

Several samples subjected to constant loading for 14 days were selected for SEM examinations. None of the sample fractured at their respective loading level. Therefore, the specimen surfaces were searched for microcracks. The selected samples are mentioned in Table 11.

Table 11. List of samples which were put in the SEM and had their surface searched for microcracks.

Sample	Corrosion protection	Applied load	Microcracks observed?
CorTest.6.s	-1050mV	95% of $\sigma_{F,S}$ for 14days	Yes
CorTest.7.s.(free)	no	95% of $\sigma_{F,S}$ for 14days	Yes
CorTest.14.s.(galv)	Zinc coating	95% of $\sigma_{F,S}$ for 14days	No
CorTest.16.s	-1050mV	100% of $\sigma_{F,S}$ for 14days	Yes
CorTest.12.s.(free)	No	100% of $\sigma_{F,S}$ for 14days	Yes
CorTest.24.s.(galv)	Zinc coating	100% of $\sigma_{F,S}$ for 14days	No

As can be observed from Table 11, no microcracks have been observed on either of the two HDG tensile specimens.

Microcracks in specimens tested at 95% of $\sigma_{F,S}$

Specimen *CorTest6.s*

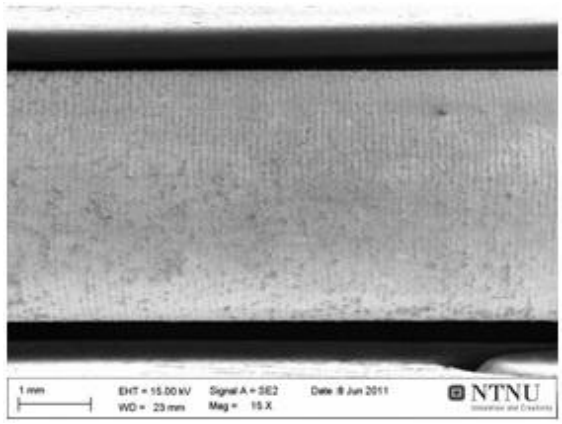

a)

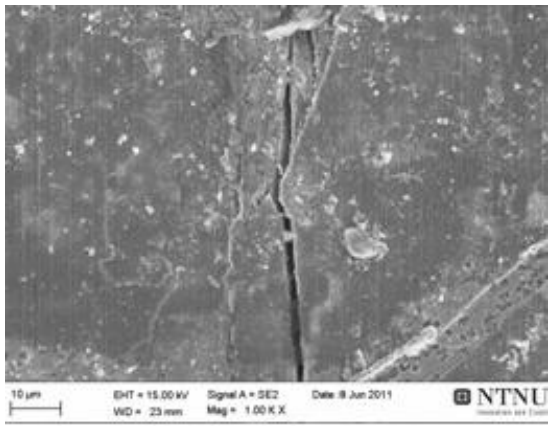

b)

Figure 38. Surface examinations of specimen *CorTest.6.s* in the SEM at; a) 15x b) 1000x at the center of the specimen.

Sample *CorTest.6.s* was loaded at 95% of 1070MPa for 14days. Examinations of the tensile specimen surface in SEM revealed microcracks. The microcracks are oriented along the machining groove on the specimen surface. No necking of the specimen could be observed.

Specimen *CorTest7.s(free)*

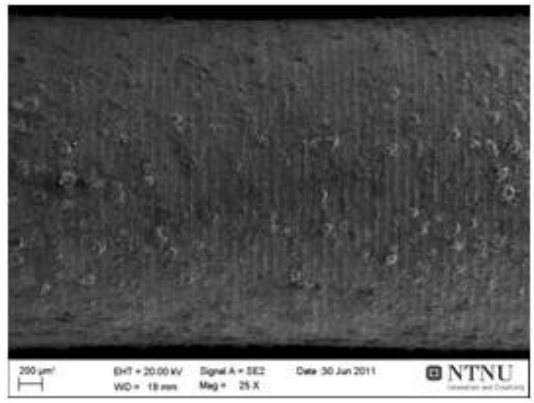

a)

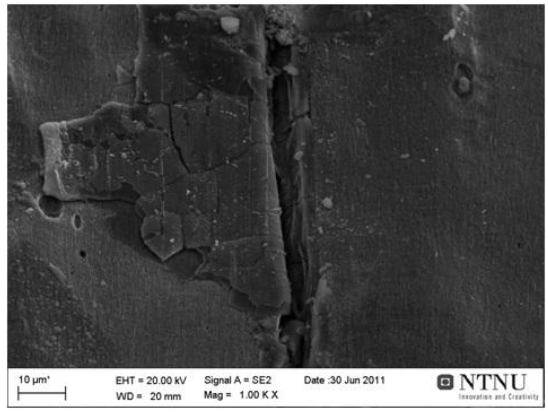

b)

Figure 39. Surface examinations of specimen *CorTest7.s(free)* in the SEM at; a) 25x, b) at 1000x the center of the sample.

Sample *CorTest7.s(free)* was loaded at 95% of 1070MPa for 14days. Examinations of the tensile specimen surface in SEM revealed microcracks. It appears like the microcracks are oriented along the machining grooves on the specimen surface.

Specimen *CorTest14.s(galv)*

Microcracks were not observed on the "damaged" test area of specimen *CorTest14s.(galv),* as seen in Figure 40.

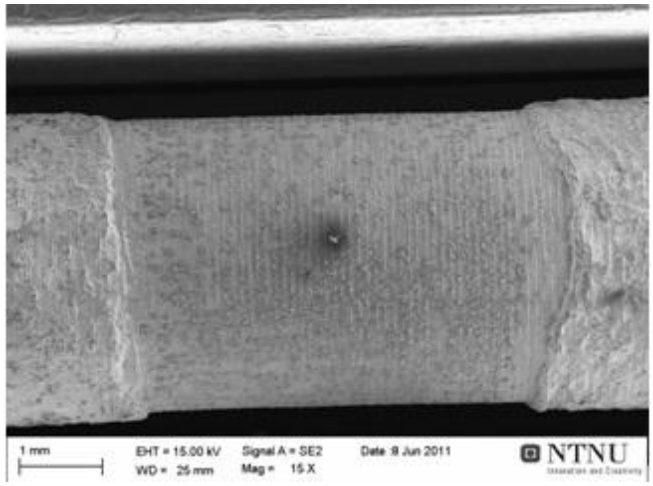

a)

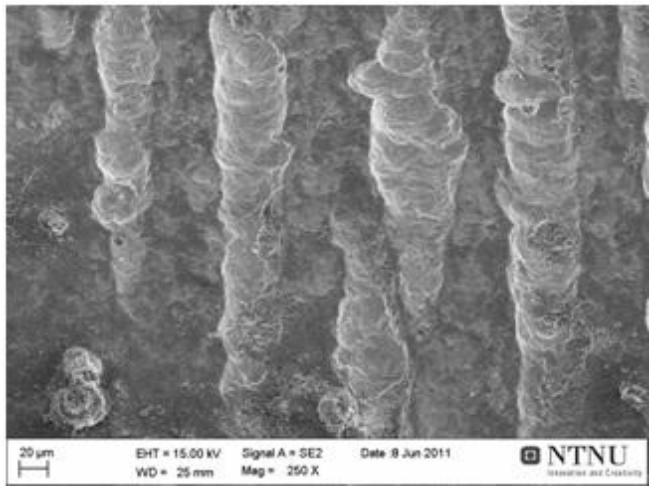

b)

Figure 40. Microcracks examinations in the SEM at; a) 15x and b) 250x.

5 Discussion

5.1 Characterization of fractured anchor chain

The fractured chain was subjected to several tests. First the microstructure was found in the light microscope. Consecutively its hardness, transition temperature and tensile curve were found. The test results are discussed in the following chapters.

5.1.1 Microstructure

The fractured chain had a lath martensittic microstructure, similar to the one found in the sandblasted chain. This was as expected as it was said that the two qualities were of the same strength class. Compared to the sandblasted chain, the microstructure of the fractured chain appears to have a finer structure. This is in agreement with the hardness measurements, were the fractured chain also is stronger than the sandblasted chain.

The light microscopic examinations did not locate any impurities or unfavorable particles in the steel. This was also the case for the sandblasted chains. Impurities are highly relevant for the materials susceptibility to HISC because they act as trap sites for the hydrogen. A good homogeneity and a low degree of contaminations in the metal would suggest that the fractured chain was fairly resistant to HISC.

5.1.2 Hardness

The hardness values for the fractured anchor chains were found to be higher than the recommendations for submerged carbons steel under cathodic protection[21]. They also exceed the recommendations from DNV RP-B401.

The hardness profile of the fractured chain according to Figure 27 was evaluated to be quite homogeneous. The fractured chain appears to have a higher degree of homogeneity than the sandblasted chain when comparing the standard deviation of the hardness measurements. The hardness profile for the bend in the transverse position was also found, and can be seen in Figure 48. No clear indication of any pattern in the hardness variations could be found. The homogeneity of the fractured chain appears to be good.

The carbon content of the fractured chain, as well as its heat treatment was unknown. It was therefore difficult to make a prediction of the hardness.

5.1.3 Charpy

The charpy curve in Figure 28 shows a material with good impact resistance. No transition temperature was found with the 9 charpy specimens. The temperature range was between -44°C to 18°C and all measured impact values was in the range of 100J. Even if no recommended values for the chain materials transition temperature is presented in the standard for chain links, NS-EN 1677-4[22], the impact strength found within the tested temperature range is considered to be good values for the environment relevant for the Norwegian coast.

The test specimens were selected from the welded side in the chain link. Due to a limited selection of fractured chain link this was all the charpy specimens it was possible to machine. Each specimen had some material loss on one end. According to the charpy standard this can be allowed as long as the contact surface between the sample and the bearing surface is at its full size.

The specimen measurements were checked prior to testing and all dimensions were within the acceptance criterion set by the standard.

5.1.4 Tensile test

When the hardness of the fractured chain was higher than the sandblasted chain, it was expected that the fractured chain would also have higher yield strength than the sandblasted chain according to the hardness conversion done by table 2.B in standard 18265[23]. However, this was not the case. The tensile test found that the yield strength of the fractured chain was 890MPa and the tensile strength was 980MPa. According to conversion table 2.B, in ISO standard 18265[23], the hardness 381HV.10 corresponds to a tensile strength of 1189MPa. This strength value is a lot higher than what was found in the tensile test. The reason for this deviation could be that the fractured chain does not fit the description of being quenched and tempered.

According to DNV-RP-B410[9], concerning *cathodic protection design,* failures caused by CP induced HISC has been encountered for martensittic steels with an yield strength of 700MPa and hardness of 350HV. The fractured chain therefore fits the description of being susceptible to HISC.

Compared to the sandblasted chain, with a fracture load of 1070MPa, the fracture load of the “fractured chain” is only 980MPa. If the fractured chain was supposed to be a grade 70 steel, it appears to be weaker than it should be. If so, the chain would be weaker than anticipated. Therefore, overload fracture could be an explanation to why the “fractured chain” failed during operation.

Typical errors in the measurements may come from machine defects. Visual inspection revealed however no surface defects.

5.1.5 Susceptibility to HISC

Based on the fact that the fractured chain was found to have a hardness and yield strength above the recommended values from DNV it would be considered susceptible to HISC. However, no inclusions or impurities were discovered in the light microscope examination. HISC related fractures are highly dependent on impurities were they act as hydrogen traps. Additionally, the microstructure is tempered martensite and not untempered martensite, which is recognized as the most dangerous martensite condition. Hence, the fractured chain appears to be of good quality with fairly good resistance to HISC.

A secondary goal of the report was to attempt to explain the reason why the fractured chain failed in-service. The minimum specified fracture load for a grade 70 chain is 700MPa. Unfortunately, the relationship between the strength of the steel and the fracture load of the chain links is not completely understood. However, the yield strength of the fractured chain was 140MPa lower than that of the sandblasted chain.

If the fractured chain was supposed to be a grade 70 steel as well, with a yield strength equal to the sandblasted chain, it may appear to be weaker than it should. The fractured chain had a tensile strength of 970MPa and yield strength of 890MPa, while the strength of the sandblasted chain was 1070MPa and 1030MPa respectively. This result implies that the fractured chain may have failed due to overload.

5.2 HISC tensile test

In the discussion an attempt will be made to determine whether the applied corrosion potentials to the chains will affect its resistance to HISC differently. Before going into the results some comments regarding the specimen design is needed. Secondly, remarks regarding the execution of the hydrogen charging of the tensile specimens will be given. Thirdly, some attention will be directed to the execution of the experiment. Thereafter, an assessment of results of the tensile test will be performed. This includes an evaluation of the fracture surfaces and the discovered microcracks.

5.2.1 Sample preparation

When preparing the tensile specimens it was discovered that the original re-galvanizing design was not compatible with the constant loading HISC rig. The reason for this was that the zinc layer placed on the thick part of the specimen, as seen on Figure 41. The additional thickness of the specimen, created by the zinc layer, made it impossible to make specimen fit into the test rig. It was necessary to remove this zinc layer on the thick part. This was done by protecting the threads and the specimens gauge section with masking tape and dipping the specimen into a solution of 10% hydrochloric acid. By masking the specimen it was possible to avoid introduction of hydrogen into the gauge section and the threads. The dipping was done for 30seconds until the heavy reaction stopped and the zinc layer had dissolved.

Figure 41. The finished product of the HDG tensile specimens.

Figure 42. Picture displaying the masking of the HDG tensile specimen before it was etched.

5.2.2 Experiment execution

Loading of hydrogen at different potentials

For most specimens the hydrogen charging was completed as planned. However, some tensile specimens experienced problems during the hydrogen charging. In Table 12 comments are given about the problems encountered during the precharging of the specimens. The specimens which did not experience problems during the hydrogen charging are not mentioned in the table.

Specimen *CorTest5.s* and *CorTest6.s* experienced a period of bad connection to the potensiostat. This probably caused the accumulated hydrogen in the specimens to be released. Therefore, the two specimens were probably not saturated with hydrogen when put into the CorTest Proof rings. Ideally the specimens would be saturated by hydrogen before being placed into HISC rig. If the specimens were saturated with hydrogen it would be more likely to initiate a brittle fracture. In the end, the mistake would not be catastrophic because the specimens were polarized to -1050mV vs. Ag/AgCl during the HISC test. The polarization ensured hydrogen would be supplied to the specimens.

Regarding the HDG specimens a white coating developed on specimens during the precharging. It was most likely a corrosion product and was expected. This coating was washed off with ethanol before the specimens were inserted into the CorTest Proof ring, so the corrosion product did not cover the exposed steel.

Table 12. Comments to the loading process of each specimen are presented.

Sample	Potential	Time	Comments
CorTest.s.3.(free)	Free corr.	10 days	No precharging
CorTest.s.25.(galv)	Free corr.	10 days	White coating developed on sample.
CorTest.s.5	-1050mV	10 days	Strong gas development on the specimen due to bad contact with ref.cell. Samples were rewashed and then replace in the rig
CorTest.s.6	-1050mV	10 days	Strong gas development on the specimen due to bad contact with ref.cell. Samples were rewashed and then replace in the rig
CorTest.s.7.(free)	Free corr.	10 days	No precharging
CorTest.s.12.(free)	Free corr.	10 days	No precharging
CorTest.s.13.(galv)	Free corr.	10 days	White coating developed on sample.
CorTest.s.14.(galv)	Free corr.	10 days	White coating developed on sample.
CorTest.s.17.(free)	Free corr.	10 days	No precharging
CorTest.s.18.(galv)	Free corr.	10 days	White coating developed on sample.
CorTest.s.24.(galv)	Free corr.	10 days	White coating developed on sample.

As mentioned in the theory more hydrogen was anticipated to be generated for the lower potentials, as per Figure 3. Most hydrogen development would be expected for the specimens subjected to -1050 mV vs. Ag/AgCl. According to the same figure however, least hydrogen would be expected at specimens without any form of corrosion protection. For the specimens without CP or a HDG layer the corrosion potential was anticipated to be in the range of -550 to -600mV vs. Ag/AgCl electrode in seawater. When the corrosion potential is in that range, the reduction of hydrogen is not expected to be the dominating reaction[6]. Less hydrogen was expected to be developed on the HDG specimens compared to the polarized specimens. Unfortunately, the amount of hydrogen absorbed in the HDG specimens compared the polarized specimens was not controlled by performing hydrogen measurements due to lack of funding.

HISC test

During the HISC test some unexpected incidents occurred for certain specimens. Comments on the matter were made for are specified for each individual specimen in the Table 13. The specimens not mentioned in the table were tested without problems.

Table 13. Comments on the progress of the HISC test for specimen subjected to unexpected incidents.

Sample	Observations
CorTest2.s	On the first day of testing, the platinum wire had fallen out of the rig and broke the connection. The specimen then corroded. Loss of hydrogen
CorTest10.s	Had problems initially with bad connection to the potensiostat causing excessive corrosion of the specimen. H was probably released. Test stopped 6 days too early
CorTest11.s	Test went according to plan. Test stopped 6 days too early
CorTest12s.(free)	Test went according to plan Test stopped 6 days too early
CorTest18.s.(galv)	Sample fractured after only 70hours. Specimen diameter was probably smaller than

The test of specimen *CorTest10.s*, *CorTest11.s,* and *CorTest12.s(free)* was stopped by a mistake after 8 of 14 days. Since the specimens were not tested like the others, they were not examined in the SEM. The specimens were therefore replaced by specimen *CorTest15.s*, *CorTest16.s,* and *CorTest17.s(free)* and tested a 100% of $\sigma_{F,S}$.

Typical sources of error made during the HISC test would be the measuring of the vertical displacements in the CorTest Proof rings. Some uncertainty will be associated to the last measured value of the vertical displacement of the CorTest Proof ring. The exact last value is difficult to pinpoint because the fracture occurs while the gripping tension is increased. The vertical displacement of the proof rings should in the future be measured automatically.

Other mistakes could be made when measurement the diameter of the threaded specimens. This is likely to be the case for specimen *CorTest18.s(galv)*. It failed earlier than expected, but SEM examination found it to be ductile. A ductile fracture could be caused by overload which indicate the applied was too high.

5.2.3 Fracture surfaces

Several fractures occurred in the HISC tensile test, but none of them were brittle. The area of reduction to fracture was use as a method to measure if the ductility was different for any of the three corrosion potentials. The measured ductility, presented in Table 10, was found be between 30-40%. The results indicate the ductility of the specimens were intact. However, the reduction of area suggest the unprotected specimens are slightly more ductile then the other fractured specimens, this is considered to be unlikely. One explanation for the reason why the un-protected specimens was found to have higher ductility could be the loss of thickness due to corrosion. Therefore, the reduction of area was higher than for those specimens which did not suffer material loss. A second explanation could be ductility variations within the material.

The succeeding discussion is divided into the tensile specimens of the fractured chain and the sandblasted chain.

Fractured chain

The two tensile specimens from the fractured chain were pulled until fracture. The exposure time of 481hours was as expected longer than the exposure time of the sandblasted chains. The tensile curve of the fractured chain, presented in Figure 33, show that the fractured material has a longer range of work hardening compared to that of the sandblasted chain, presented in Figure 47. It was therefore expected that the specimens would take longer to fracture since the applied load was increased in steps.

The fracture load was reached at 110% of the materials yield strength. That means the fracture load was equal to the materials tensile strength of 980MPa. However, it could be that the real load on the specimen was higher because of necking.

All of the fractographic images point towards ductile fractures, which can be observed by the dimples in the pictures in Figure 34. Introduced hydrogen had not embrittled the steel.

Sandblasted chain

The CorTest generated fracture in several sandblasted specimens. *CorTest1.s*, *CorTest2.s*, *CorTest.s.25.(galv)*, *CorTest3s.(free) and CorTest15.s* were deliberately pulled until fracture.

Specimen *CorTest18s.(galv)* was the only specimen not pulled to fracture deliberately. It fractured after 70.7 hours under a tension load of 1070MPa. Since it was the only specimen to fracture prematurely, it was believed to be embrittled by the hydrogen. However, examinations in the SEM revealed a ductile fracture surface, as seen in Figure 51. The fracture surface was purely covered with dimples. After 70hours is was discovered that the applied load on specimen C*orTest18.s(galv)* was too low. The applied load was consequently increased to the correct level. While increasing the load, the specimen fractured. One explanation could be that this particular specimen was weaker that the measured tensile strength of 1070MPa. Another explanation could be that the measured cross section was smaller than the actual cross section. The latter cannot be discarded due to the human factor during measuring.

The exposure time of specimen *CorTest25s.(galv)* in the CorTest Proof ring was measured to be 604hours, and did not fracture until a force of approximately 110% of the material yield strength was reached. The measured time is unfortunately higher than it should have been. While in the test rig, the specimen was forgotten and left in the rig for 2 days extra between the second last and last increase in gripping tension.

All of the fracture surfaces of the sandblasted tensile specimens are coved with dimples, indicating that the material was ductile. The measured area of reduction was nearly equal for all of the sandblasted specimens. Even if more hydrogen is developed on polarized tensile specimens, it appears to have no effect on the sandblasted steels ductility.

5.2.4 Microcracks

The surface of the sandblasted tensile specimens, which did not fracture during their respective constant loads, was investigated for microcracks. The results can be found in Table 11. One specimen from each type of load and corrosion potential was examined in the SEM.

Regarding specimen *CorTest5.s* and *CorTest6.s,* no brittle fracture was not provoked. Even after the specimen lost its accumulated hydrogen during the hydrogen charging, enough hydrogen was present at the applied load to assist the development of microcracks on the specimens. This indicates that the material did not need to be fully saturated with hydrogen to crack. Consequently, the material is not completely resistant to HISC when polarized to -1050mV vs. Ag/AgCl.

The un-protected specimens were expected to corrode at a potential of roughly -600mV vs. Ag/AgCl. Here, hydrogen development was not expected be the dominating reduction reaction. For solutions with pH larger than 3.5 (here 6.5) the oxygen reduction reaction will dominate over the hydrogen reduction[6]. The loss of specimen thickness during loading may have increased the forces acting on the specimen, and consequently cause cracking.

From the results in Table 11 it was found that the HDG specimens had not developed microcracks for any of the applied loads. This was believed to be connected to the relation in Figure 3, where less hydrogen

evolution was expected at a potential of -900mV vs. Ag/AgCl compared to a potential of -1050mV vs. Ag/AgCl. The reason why no cracking occurred at the HDG specimens can therefore be a consequence of too little available hydrogen. The HDG specimens seem resistant to HISC, since the applied loads and the imposed levels of hydrogen did not generate brittle failure or cracking.

Both the specimens set to corrode freely, and the specimens protected by a potential of -1050mV against Ag/AgCl, had developed microcracks. For the polarized specimen, the microcracks can initiate HISC. The cracks in the unprotected specimen however, cannot initiate HISC because of small hydrogen develop at the respective corrosion potential.

There was a tendency for the microcracks to be orient along the machining grooves on the specimen surface. As expected, cracks tend to form at stress concentrations. This is comparable to the case in the fishing industry were chains failed in-service[3]. In that case the fracture occurred at the in the bend of the chain, where chain meets chain. Here, high triaxial stresses act and relative movement between the contact faces wear down the HDG layer.

Can it be document that the amount of hydrogen present influences the amount of cracking of the specimen? Results point towards yes. The highest amount of cracking was found in the polarized tensile specimens, which also was anticipated to be exposed to the highest amount of hydrogen evolution.

For future reference the size of the microcracks on the specimens should be measured. Unfortunately there was no time left to measure the depth of the surface microcracks or to search for internal microcracks in the specimens.

5.2.5 Effect of hydrogen during tensile testing

The HISC test is a good technique to examine the susceptibility of the anchor chain steel to HISC. However, the test circumstances are a simplification of the reality. The forces that act on the full scale chains in use are dynamic and unpredictable, unlike the test conditions applied in our experiment. Also one should take into consideration the tribo-corrosion aspect present when the chains are in use. In-service the chain-vs-chain friction and relative movement will wear down the zinc coating in the contact points of the linking chain rings. From the theory it is known that wear and corrosion have a synergetic effect which leads to high corrosion rates. As a recommendation for future work, a full scale submerged tensile test should be performed on connected chain links to address this issue.

The hydrogen imposed on the specimens during the HISC test do not seem to be able to have an embrittling effect on the base material in the chain. However, microcracks had developed at stress levels below the yield strength, in verification phase 2, for the un-protected and steel polarized to -1050mV vs. Ag/AgCl. Microcracks also develop at the higher loads, in verification phase 3.B, on the un-protected steel and polarized steel. The microcracks on the polarized specimens indicate that HISC may be initiated. It is therefore recommended to keep the HDG layer as a corrosion protection, as no microcracks were generated when it was applied. Nevertheless, no loss of ductility was experienced for any of the tensile specimens in the HISC test, as seen from Table 10. The area of reduction was similar for all the specimens, regardless of applied load and corrosion potential, with the exception of the un-protected specimens. Additionally HDG specimen seems to be fully resistant to HISC. Hence, the hydrogen seem to have no effect on the mechanical properties of the HDG sandblasted steel, while for the polarized specimens the hydrogen appear to assist in cracking.

6 Conclusion

A fractured anchor chain of an unknown origin was characterized in terms of its microstructure, hardness, hardness profile, transition temperature and strength. The following results were generated;

- The fractured chain had a lath martensittic structure in the tempered condition.
- Average hardness: 381 ± 8 HV
- No transition temperature was discovered in the charpy test in the temperature range of <-44°C, 18°C >.
- Yield strength: 890MPa
- Tensile strength: 980MPa

Compared to the sandblasted chain, the yield strength of the fractured chain was 140MPa lower. If the two chain qualities were supposed to be of equal strength, the fractured chain could have failed in-service due to overload because it was weaker than promised.

The fractured chain was compared to a sandblasted grade 70 anchor chain in terms of its susceptibility to HISC. This was tested by precharging tensile specimens with hydrogen and performing a submerged constant load test in CorTest Proof rings for 14 days while they were exposed to hydrogen at different corrosion potentials.

- No brittle fractures were provoked by the conditions used in the HISC test.
- Cracking was pronounced for unprotected specimens and specimens polarized to -1050mV vs. Ag/AgCl.
- Cracking was not observed on HDG specimens with the applied tensile stresses and the amount of hydrogen present during the test

The HDG, sandblasted tensile specimens appear resistant to HISC as no loss in ductility takes place and no microcracks were observed on any of the specimens' surfaces.

7 Recommendations for further work

It should be conducted an elemental analysis of the fractured steel and of the sandblasted steel to verify the alloying elements according to their respective material certificate. When the composition is known it can be evaluated according to the use of the chain if it is suitable to the application. Regarding the chemical composition of the sandblasted chain there is reason to doubt the values mentioned in the material certificate, since the mechanical properties mentioned there were proven to be incorrect. The chemical composition of the fractured chain was also unknown.

Some tensile specimens were not examined in the SEM. Remaining fracture surfaces should be characterized, and specimens which did not fracture should be examined for microcracks.

One should do an evaluation of the costs of the lifecycle of the chain material if it is to be used. It would require extra efforts of monitoring and maintenance. Perhaps one must consider the need for reducing the in-service lifetime of the chain and change steel chains during the design lifetime of the fish farming facility.

There was no time to look for microcracks in the cross section of the non-fractured tensile specimens. Cross sectional or longitudinal examinations should be performed in SEM and the depth and size of potential cracks should be measured.

Additionally, on the basis of the chain rings geometry and base material one can perform a FEM-analysis of the deformation of a chain at different loading levels. The results can be compared towards practical tests. Tensile tests can for example be performed on full sized linked chain rings. By obtaining this kind of information it can be possible to determine the relationship between the strength of the base material and the fracture load of the chain links.

Reference list

1. Dahle, K.O., J.K. Solberg, and R. Johnsen, Characterization of grade 70 steel used in anchoring chains in the fishing industry. 2010, NTNU: Trondheim.
2. Norman, M. and H.F. Høydahl, Lenken som brast, in VG. 2010, VG Multimedia: Oslo. p. 16-21.
3. Force Technology, Brudd i kjetting ved oppdrettsanlegg for fisk, Fiskeridirektoratet på vegne av rømmingskommisjonen for akvakultur, Editor. Sept 2009: Trondheim.
4. Standard Norge, ISO 21457:2010, in Petroleumsindustri, petrokjemisk industri og naturgassindustri. Materialvalg og korrosjonskontroll for olje- og gassproduksjonssystsemer. 2010.
5. Johnsen, R., Cathodic Protection. September 2008, NTNU: Trondheim. p. 27.
6. Bardal, E., Korrosjon og korrosjonsvern. 2 ed. Vol. 2.utgave. 1994, Trondheim: Tapir Akademiske Forlag.
7. Colangelo, V.J. and F.A. Heiser, Analysis of metallurgical failure. Second edition ed. 1987: John Wiley & Sons, Inc.
8. Mikkelsen, B.D., Hydrogen Embrittlement in Super Duplex Stainless Steel, in Course 41652 Metals Technology. April 2009,, DTU Mekanik - Institut for Mekanisk Teknologi: Copenhagen.
9. Veritas, D.N., Cathodic Protection Design, in Recommended Practice
DNV-RP-B401. 2010.
10. Fontana, M.G. and N.D. Greene, Environmental Induced Cracking, in Corrosion Engineering. 1967, McGraw-Hill: New York.
11. Olden, V., C. Thaulow, and R. Johnsen, Modelling of hydrogen diffusion and hydrogen induced cracking in supermartensitic and duplex stainless steels. Materials & Design, 2008. 29(10): p. 1934-1948.
12. Solberg, J.K., Subject: Analysis of Metallurgical Failure - Hydrogen Degradation. 2011, NTNU: Trondheim.

13. Askeland, D.R. and P.P. Phulé, The science and Engineering of Materials. 5th ed. 2006: Thomson.
14. Anderson, T.L., Fracture Mechanics, fundamentals and applications. Third edition ed. 2005: CRC Press.
15. Eliaz, N., et al., Characteristics of hydrogen embrittlement, stress corrosion cracking and tempered martensite embrittlement in high-strength steels. Engineering Failure Analysis, 2002. 9(2): p. 167-184.
16. Erling Haug AS. 2010; Picture and table showing the dimensions and the design of the chain ring to undergo metallurgical investigation]. Available from: http://katalog.haug.no/sortrondelag/trondheim/ehaug/produktkatalog.nsf/.
17. Bailey, J.A., Mechanical Testing and Evaluation, in ASM Handbook. 2003.
18. Marson, A., Work procedure for hydrogen loading of specimens. 2011, Sintef: Trondheim. p. 6.
19. NACE, TM0177-96, in Laboratory Testing of Metals for Resistance to Sulfide Stress Cracking in Hydrogen Sulfide (H2S) Environments. 1996, NACE International.
20. Lange, T., O.Ø. Knudsen, and B.W. Tveiten, General description of the working procedure for - Constant Load Testing. 2007, Sintef Materials and Chemistry,Sintef Materials and Chemistry Trondheim.
21. Det Norske Veritas, Cathodic Protection Design. January 2005.
22. Standard, N., Components for slings - Safety, in Part 4: Links, Grade 8. 2000, Standard Norge.
23. Norsk Standard, NS-EN ISO 18265, in Metalliske materialer - omregning av hardhetsverdier. 2004, Standard Norge,.

Appendix A – Previous work

Test results from the previous project work on the sandblasted steel is presented[1].

Attachment A.1 – Microstructure of the sandblasted chain

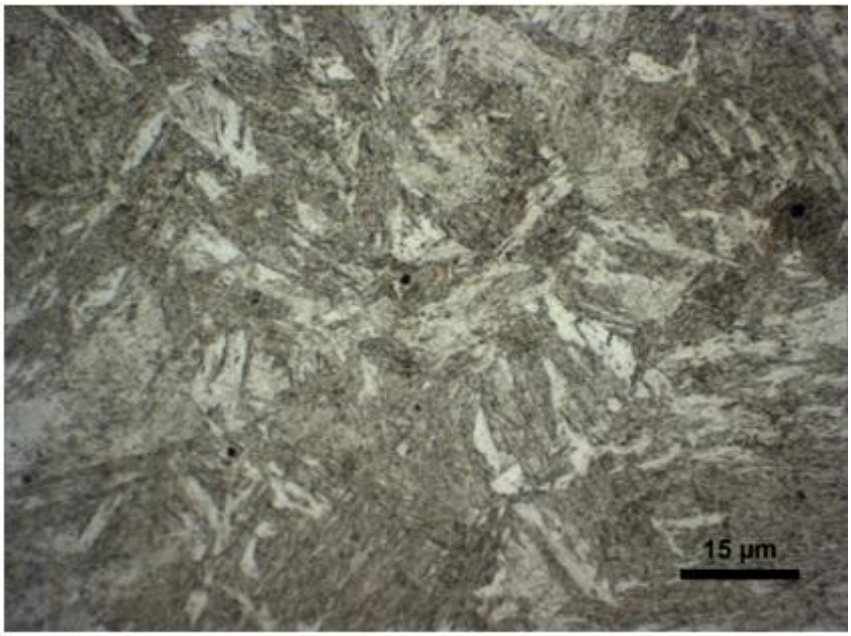

Figure 43. Microstructure of the sandblasted chain.

The microstructure of the sandblasted chain is a lath martensittic type, and appears to be in the tempered condition.

Attachment A.2 – Hardness profiles for the sandblasted chain.

The average hardness of the sandblasted chain was 367 ±12 HV.10. The hardness profiles of the chain is presented in the Figure 44 and Figure 45.

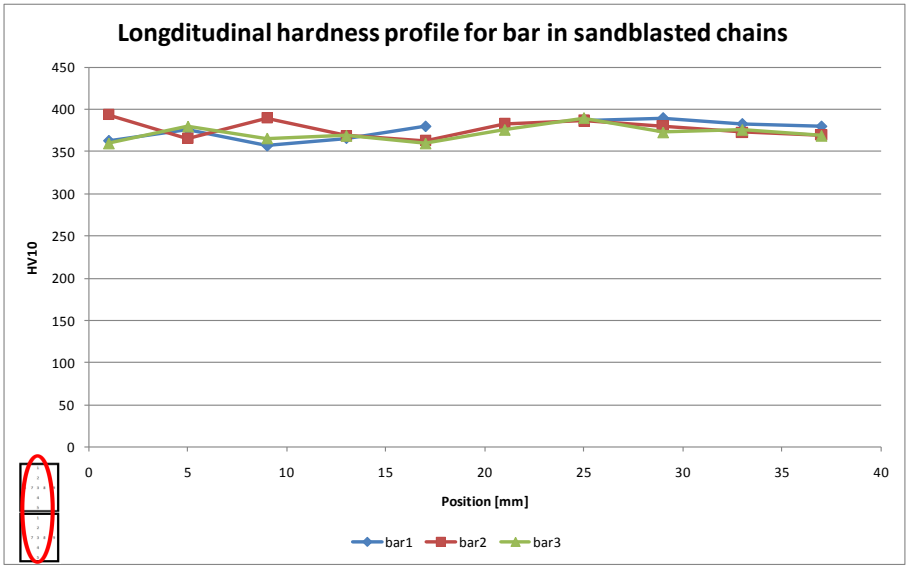

Figure 44. Longitudinal hardness profile for the bar in three sandblasted chain rings.

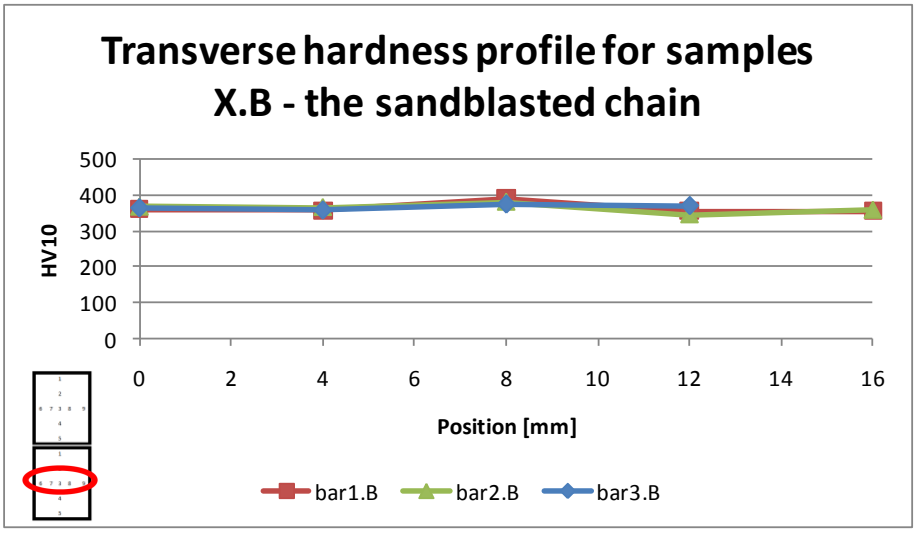

Figure 45. Transverse hardness profile for the sandblasted chains.

Attachment A.3 – Charpy results

The transition temperature was determined to -11°C.

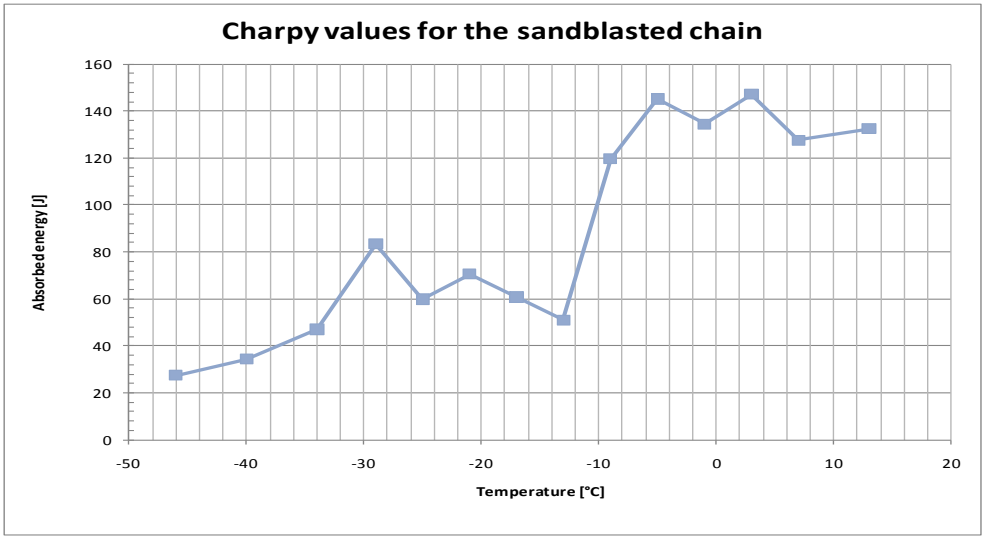

Figure 46. Charpy values for the sandblasted chain. Samples are taken from the unwelded part of the chain ring.

Attachment A.4 – Stress-strain curve of the sandblasted steel

The yield strength of the sandblasted chain is 1030MPa while the tensile strength was 1070MPa. Elongation to fracture varied from 12.6% to 13.8%.

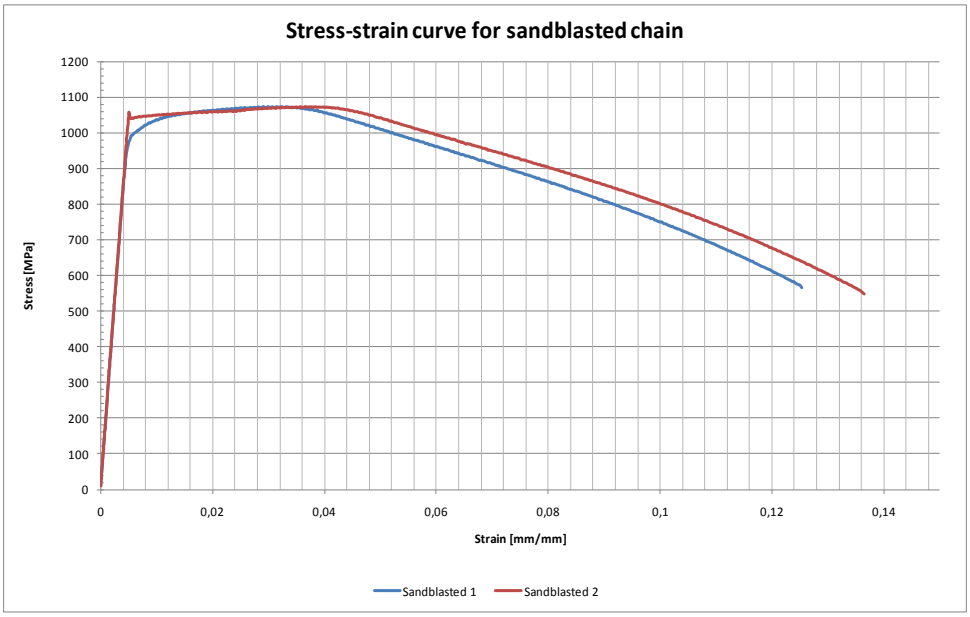

Figure 47. Stress strain curve for the sandblasted chain.

Appendix B – Experimental results

Attachment B.1 – Hardness

The transverse hardness profile of the fractured anchor chain was found and is presented in Figure 48.

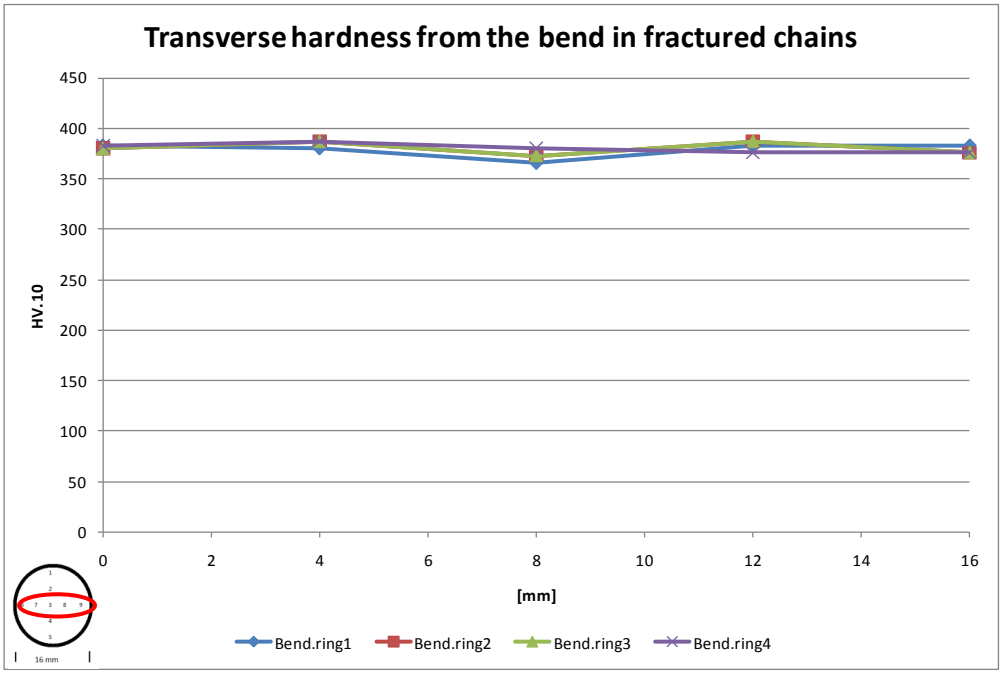

Figure 48. Transverse hardness profile from the bend in fractured chains.

Table 14. Measurements and values for the sandblasted hardness specimens 1.T.c, 2.T.a, 3.T.c, 4.T.a.

Bend.ring 1

Sample 1 1.T.c

Position #	D.1[µm]	D.2[µm]	HV.10
1	218.4	216.2	394
2	221.0	223.0	380
3	225.4	224.9	366
4	217.0	217.1	394
5	222.2	220.6	380
6	219.8	221.2	383
7	220.9	220.3	380
8	220.0	220.0	383
9	219.7	220.9	383

Bend.ring 2

Sample 2 2.T.a

Position #	D.1[µm]	D.2[µm]	HV.10
1	223.5	222.2	373
2	217.7	217.8	390
3	222.3	223.0	373
4	219.9	221.1	380
5	215.6	215.6	397
6	221.3	220.2	380
7	219.6	218.3	387
8	218.1	219.5	387
9	220.7	223.1	376

Bend.ring 3

Sample 3 3.T.c

Position #	D.1[µm]	D.2[µm]	HV.10
1	223.6	228.7	373
2	220.8	226.7	390
3	219.0	222.7	373
4	216.8	217.5	380
5	222.0	223.4	397
6	224.0	219.2	380
7	219.6	218.9	387
8	220.4	220.1	387
9	223.4	220.2	376

Bend.ring 4

Sample 4 4.T.a

Position #	D.1[µm]	D.2[µm]	HV.10
1	221.6	218.5	363
2	217.8	217.3	369
3	223.7	223.3	380
4	222.7	222.7	394
5	220.4	220.4	373
6	225.6	219.5	383
7	219.9	216.8	387
8	219.4	218.8	376
9	219.2	216.3	376

Attachment B.2 – Charpy values

The results from the charpy test conducted on the fractured anchor chain are presented in Table 15.

Table 15. Charpy values and measurements for the sandblasted and the fractured anchor chain.

Fractured chain

Chain #	Sample #	Temp [°C]	Impact energy [kgm]	Impact strength [J]
1	1	18	10.7	105.0
1	2	8	10.8	105.9
1	3	0	10.8	105.9
1	4	-6	11.2	109.9
2	5	-12	9.8	96.1
2	6	-18	9.9	97.1
3	7	-24	9.9	97.1
3	8	-36	8.7	85.3
4	9	-44	10.9	106.9

Attachment B.3 – HISC testing program

The test program for the HISC rig is presented in Table 16 and Table 17.

Table 16. Sample numbering and test program for the sandblasted anchor chains.

Chain #	Sample	HDG	Test parameter	Load
1	CorTest1.s	no	-1050mV	90% of σ_Y + 2% increase/2.day until fracture
2	CorTest2.s	no	-1050mV	90% of σ_Y + 2% increase/2.day until fracture
3	CorTest3.s	no	Free potential	90% of σ_Y + 2% increase/2.day until fracture
25	CorTest25.s(galv)	yes	-1050mV	90% of σ_Y + 2% increase/2.day until fracture
5	CorTest5.s	no	-1050mV	95% of σ_F for 14days
6	CorTest 6.s	no	-1050mV	95% of σ_F for 14days
7	CorTest7.s.(Free)	no	Free potential	95% of σ_F for 14days
10	CorTest10.s	no	-1050mV	100% of σ_F for 14days
11	CorTest11.s	no	-1050mV	100% of σ_F for 14days
12	CorTest12.s.(free)	no	Free potential	100% of σ_F for 14days
13	CorTest13.s.(galv)	yes	Free potential	95% of σ_F for 14days
14	CorTest14.s.(galv)	yes	Free potential	95% of σ_F for 14days
15	CorTest15.s	no	-1050mV	100% of σ_F for 14days
16	CorTest16.s	no	-1050mV	100% of σ_F for 14days
17	CorTest17.s.(free)	no	Free potential	100% of σ_F for 14days
18	CorTest18.s.(galv)	yes	Free potential	100% of σ_F for 14days
24	CorTest24.s.(galv)	Yes	Free potential	100% of σ_F for 14days
19	hisc19	yes	-	Extra
20	hisc20	Yes	-	Extra
21	hisc21	Yes	-	Extra
22	hisc22	Yes	-	Extra
23	hisc23	Yes	-	Extra

Table 17. Sample dumbering and test program for the "fractured" anchor chain.

Chain #	Sample	HDG	Test parameter	Load
3	CorTest1.f	no	-1050mV	90% of σ_Y + 2% increase/2.day until fracture
4	CorTest 2.f	no	-1050mV	90% of σ_Y + 2% increase/2.day until fracture

Attachment B.4 – Calculations of gripping tension for HISC testing of the fractured chains

Specimens were initially loaded at 90% of $\sigma_{Y,F}$. The yield strength of the fractured chain was found to be 890MPa, while the tensile strength was 980MPa. The calculations were made in an Excel work sheet prepared by lab-engineers at Sintef were the experiments were conducted.

Table 18. Data for calculating gripping tension for the HISC test of the fractured chains.

Data:			
Yield strength	YS =	890	MPa
% of YS		90	%
90 % av flyt		801	MPa

Sample marking	Diameter	Cell No	Calibration Curve Const 1	Const 2	Displacement mills	mm
	(mm)		Stiff ring			
	0.00	2622	91008,7174	-95,3923	0.00	0.00
	0.00	2623	88062,4857	-131,3047	0.00	0.00
	0.00	2628	90396,4741	-73,8678	0.00	0.00
CorTest1.f	3.73	2629	92389,4493	-130,4243	22.71	0.57
CorTest2.f	3.75	2630	89550,5217	-100,2199	23.33	0.59

mm - inches	25,4	lbs - Newton	0,224
Newton - lbs	4,448		

The displacement distance of the Proof rings in is measured against the default height of the proof ring, h_0. Each cell has its own h_0. These heights can be found in Table 5 in chapter 3.3.6.

Example: For CorTest1.f.
Default height of cell number 2629 is 219,21mm. Initial displacement is 0.59mm. The new $h_1 = h_0 +$ Displacement.
h_1 = (219.21 – 0.59) mm = 218.62 mm.

Attachment B.5 – Loading scheme for fractured chains.

Table 19. Fractured tensile specimens were first exposed to a load of 90% of its yield strength. Consequently, the load was increased by 2% of its yields strength pr. second day until fracture.

Number of days:		2
% of $\sigma_{Y,F}$:		92
Sample	**Distance**	**Hours**
CorTest1.f	218,62	48
CorTest2.f	218,61	48

Number of days:		4
% of $\sigma_{Y,F}$:		94
Sample	**Distance**	**Hours**
CorTest1.f	218,61	96
CorTest2.f	218,59	96

Number of days:		6
% of $\sigma_{Y,F}$:		96
Sample	**Distance**	**Hours**
CorTest1.f	218,60	144
CorTest2.f	218,58	144

Number of days:		8
% of $\sigma_{Y,F}$:		98
Sample	**Distance**	**Hours**
CorTest1.f	218,59	192
CorTest2.f	218,57	192

Number of days:		10
% of $\sigma_{Y,F}$:		100
Sample	**Distance**	**Hours**
CorTest1.f	218,57	240
CorTest2.f	218,55	240

Number of days:		12
% of $\sigma_{Y,F}$:		102
Sample	**Distance**	**Hours**
CorTest1.f	218,56	288
CorTest2.f	218,54	288

Number of days:		14
% of $\sigma_{Y,F}$:		104
Sample	**Distance**	**Hours**
CorTest1.f	218,55	336
CorTest2.f	218,53	336

Number of days:		16
% of $\sigma_{Y,F}$:		106
Sample	**Distance**	**Hours**
CorTest1.f	218,53	384
CorTest2.f	218,52	384

Number of days:		18
% of $\sigma_{Y,F}$:		108
Sample	**Distance**	**Hours**
CorTest1.f	218,52	432
CorTest2.f	218,50	432

Number of days:		20
% of $\sigma_{Y,F}$:		110
Fracture load (MPa):		979
Sample	**Distance**	**Hours**
CorTest1.f	Fracture	481,2
CorTest2.f	Fracture	481,2

Attachment B.6 – Calculations of gripping tension for screening samples in the HISC test

The first specimens to be pulled worked as a screening to find the fracture limit of the steel under the test conditions. Samples were initially loaded at 90% of $\sigma_{Y,S}$. The yield strength of the fractured chain was found to be 1030MPa, while the tensile strength was 1070MPa. As can be observed from the table below the initial load for sample *CorTest1.s*, *CorTest2.s* and *CorTest3.s(free)* was too low. Sample *CorTest25.s.(galv)* was also loaded with an incorrect initial load of 90% of 1010MPa instead of 1030MPa. This was due to a calculation mistake. After two days the load was corrected from 90% of $\sigma_{Y,F}$ to 90% of $\sigma_{Y,S}$

Table 20. Data for calculating the gripping tension for sandblasted tensile specimens in the screening phase.

Data:			
Yield Strength	YS =	890	MPa
% of YS		90	%
90 % of yield		801	MPa

Data: for CorTest25s.galv			
Yield Strength	YS =	1010	MPa
% of YS		90	%
90 % of yield		900	MPa

Sample marking	Diam.	Cell No	Calibration Curve Const 1	Const 2	Displacement mills	mm
	(mm)		Stiff ring			
CorTest1.s	3,70	2622	91008.7174	-95,3923	22.32	0.56
CorTest2.s	3,71	2623	88062.4857	-131,3047	23.60	0.60
CorTest3.s.free	3,87	2628	90396.4741	-73,8678	24.25	0.61
CorTest25s.galv	3,67	2629	92389.4493	-130,4243	24.81	0.63
		2630	89550.5216	-100,2199	0,00	0,00

mm - tommer	25,4	lbs - Newton	0,224
Newton - lbs	4,448		

Attachment B.7 – Loading scheme for the sandblasted screening samples

Table 21. Samples were first exposed to a load of 90% of its yield strength. Consequently the load was increased by 2% of its yields strength pr. second day until fracture.

Number of days:		2
% of $\sigma_{Y,S}$:		90(92)
Sample	**Distance**	**Hours**
CorTest1.s	218.57mm	48
CorTest2.s	218.42mm	
CorTest3.s(free)	218.53mm	48
CorTest25.s(galv)	218.57mm	(48)

Number of days:		4
% of $\sigma_{Y,S}$:		92(94)
Sample	**Distance**	**Hours**
CorTest1.s	218.56mm	96
CorTest2.s	218.40mm	96
CorTest3.s(free)	218.51mm	96
CorTest25.s(galv)	218.56mm	(96)

Number of days:		6
% of $\sigma_{Y,S}$:		94(96)
Sample	**Distance**	**Hours**
CorTest1.s	218.54mm	144
CorTest2.s	218.39mm	144
CorTest3.s(free)	218.50mm	144
CorTest25.s(galv)	218.54mm	(144)

Number of days:		8
% of $\sigma_{Y,S}$:		96(98)
Sample	**Distance**	**Hours**
CorTest1.s	218.53mm	192
CorTest2.s	218.37mm	192
CorTest3.s(free)	218.48mm	192
CorTest25.s(galv)	218.53mm	(192)

Number of days:		10
% of $\sigma_{Y,S}$:		98(100)
Sample	**Distance**	**Hours**
CorTest1.s	218.52mm	240
CorTest2.s	218.36mm	240
CorTest3.s(free)	218.46mm	240
CorTest25.s(galv)	218.51mm	(240)

Number of days:		12
% of $\sigma_{Y,S}$:		100(102)
Sample	**Distance**	**Hours**
CorTest1.s	218.50mm	288
CorTest2.s	218.34mm	288
CorTest3.s(free)	218.45mm	288
CorTest25.s(galv)	218.50mm	(288)

Number of days:		14
% of $\sigma_{Y,S}$:		102(104
Sample	**Distance**	**Hours**
CorTest1.s	218.49mm	336
CorTest2.s	218.33mm	336
CorTest3.s(free)	218.43mm	336
CorTest25.s(galv)	218.49mm	(336)

Number of days:		16
% of $\sigma_{Y,S}$:		104(106)
Sample	**Distance**	**Hours**
CorTest1.s	218.47mm	384.0
CorTest2.s	218.31mm	384.5
CorTest3.s(free)	Fracture	385.2
CorTest25.s(galv)	218.47mm	(384)

Number of days:		18
% of $\sigma_{Y,S}$:		106(108)
Sample	**Distance**	**Hours**
CorTest1.s	218.46mm	432.0
CorTest2.s	Fracture	434.3
CorTest3.s(free)	Fracture	385,2
CorTest25.s(galv)	218.46mm	(432)

Number of days:		20
% of $\sigma_{Y,S}$:		108(110)
Sample	**Distance**	**Hours**
CorTest1.s	Fracture	483.2
CorTest2.s	Fracture	434.3
CorTest3.s(free)	Fracture	385,2
CorTest25.s(galv)	218.44mm	(480)

Number of days:		25
% of $\sigma_{Y,S}$:		(112)
Sample	**Distance**	**Hours**
CorTest1.s	Fracture	483.2
CorTest2.s	Fracture	434.3
CorTest3.s(free)	Fracture	385.2
CorTest25.s(galv)	Fracture	(602)

Comments:

For *CorTest25.s(galv)* the sudden increase in time between the second last(day 20) and last (day 25) of loading occurred because the specimen was undeliberately loaded for two extra days.

Attachment B.8 – Calculations of gripping tension for sandblasted samples subjected to constant loading at 95% of $\sigma_{F,S}$ in the HISC test

Data:		
Tensile Strength TS =	1070	MPa
% of TS	95	%
95 % of the TS	1016.5	MPa

Sample marking	Diameter	Cell No	Calibration curve Const 1	Const 2	Displacement mills	mm
	(mm)		Stiff ring			
CorTest5.s	0.70	2622	91008.7174	-95.3923	28.19	0.71
CorTest6.s	0.71	2623	88062.4857	-131.3047	28.94	0.73
CorTest7.s(free)	0.74	2628	90396.4741	-73.8678	28.94	0.76
		2629	92389.4493	-130.4243	0.00	0.00
		2630	89550.5216	-100.2199	0.00	0.00

Sample marking	Diameter	Cell No	Calibration curve Const 1	Const 2	Displacement mills	mm
	(mm)		Stiff ring			
CorTest13.s.(galv)	3,73	2622	91008.7174	-95.3923	28.49	0.72
CorTest14.s.(galv)	3,81	2623	88062.4857	-131.3047	31.08	0.79
		2628	90396.4741	-73.8678	0.00	0.00
		2629	92389.4493	-130.4243	0.00	0.00
		2630	89550.5216	-100.2199	0.00	0.00

Attachment B.9 – Loading scheme for the sandblasted tensile samples at 95% of $\sigma_{F,S}$

Number of days:		14
% of $\sigma_{F,S}$:		95
Load		1016,5
Sample	**Distance**	**Hours**
CorTest5.s	218.50	363.9
CorTest6.s	218.36	363.2
CorTest7.s(free)	218.46	361.0
CorTest13.s(galv)	218.49	330.5
CorTest14.s(galv)	218.30	330.3

Attachment B.10 – Calculations of gripping tension for sandblasted samples subjected to constant loading at 100% of $\sigma_{F,S}$ in the HISC test

Data:			
Tensile Strength	TS =	1070	MPa
% of TS		100	%
100 % av flyt		1070	MPa

Sample marking	**Diam.**	**Cell No**	**Calibration curve Const 1**	**Const 2**	**Displacement mills**	**mm**
	(mm)		Stiff ring			
CorTest10.s	3.69	2622	91008.7174	-95.3923	29.32	0.74
CorTest11.s	3.71	2623	88062.4857	-131.3047	31.02	0.79
CorTest12.s.(free)	3.70	2628	90396.4741	-73.8678	29.43	0.75
CorTest18.s.(galv)	3.88	2629	92389.4493	-130.4243	32.20	0.82
CorTest24.s.(galv)	3.74	2630	89550.5216	-100.2199	30.63	0.78
CorTest15.s	3.67	2622	91008.7174	-95.3923	29.01	0.74
CorTest16.s	3.79	2623	88062.4857	-131.3047	32.31	0.82
CorTest17.s.(free)	3.52	2628	90396.4741	-73.8678	26.71	0.68

Attachment B.11 – Loading scheme for the sandblasted tensile samples at 100% of $\sigma_{F,S}$

Table 22. Samples were first exposed to a load of 100% of its tensile strength for 14 days, with a few exceptions.

Number of days:		4
% of $\sigma_{F,S}$:		100
Load [MPa]		1070
Sample	**Distance**	**Hours**
CorTest10.s	218,47mm	96.0
CorTest11.s	218,30mm	96.0
CorTest12.s.(free)	218,47mm	96.0
CorTest18.s.(galv)	Fracture	70.7
CorTest24.s.(galv)	218,43mm	96.0
CorTest15.s	218,48mm	96.0
CorTest16.s	218,26mm	96.0
CorTest17.s.(free)	218,54mm	96.0

Number of days:		8
% of $\sigma_{F,S}$:		100
Load [MPa]		1070
Sample	**Distance**	**Hours**
CorTest10.s	Stopped	195,2
CorTest11.s	Stopped	194,6
CorTest12.s.(free)	Stopped	195,6
CorTest24.s.(galv)	218.43mm	192
CorTest15.s	218.48mm	192
CorTest16.s	218.26mm	192
CorTest17.s.(free)	218.54mm	192

Number of days:		14
% of $\sigma_{F,S}$:		100
Load [MPa]		1070
Sample	**Distance**	**Hours**
CorTest24.s.(galv)	Stopped	336.1
CorTest15.s	218.48mm	336.0
CorTest16.s	Stopped	363.5
CorTest17.s.(free)	218.54mm	336.0

Number of days:		15
% of $\sigma_{F,S}$:		100
Load [MPa]		1091
Sample	**Distance**	**Hours**
CorTest15.s	Fracture	364.0
CorTest17.s.(free)	218.54mm	360.0

Number of days:		17
% of $\sigma_{F,S}$:		100
Load [MPa]		1091
Sample	**Distance**	**Hours**
CorTest17.s.(free)	Fracture	406.7

Attachment B.12 – Fracture surfaces in the SEM

CorTest15.s

Specimen *CorTest15.s* was first subjected to constant load equivalent to 100% of its tensile strength/ fractured load. After the two week period the load was increased by 5% of its tensile strength/ fractured load. The specimen fractured during the load increase.

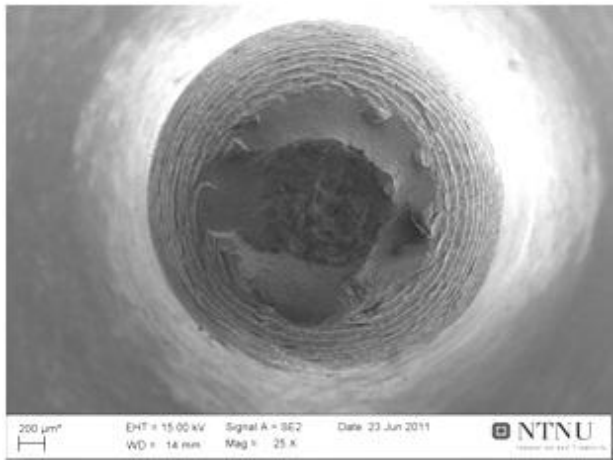

a)

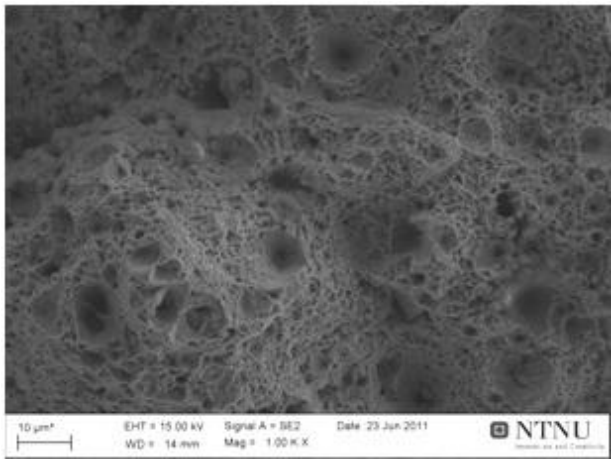

b)

Figure 49. a) Macroscopic view of the tensile specimen *CorTest15.s* of the fractured chain at 25x. b) Fractographic photo of the center of sample *CorTest15.s* at 1000x with dimples.

The fracture surface is coved with dimples indicating a ductile fracture.

CorTest17.s(free)

Specimen *CorTest17.s(free)* was first subjected to constant load equivalent to 100% of its tensile strength/ fractured load. After the two week period the load was increased by 5% of its tensile strength/ fractured load. The specimen fractured during the load increase.

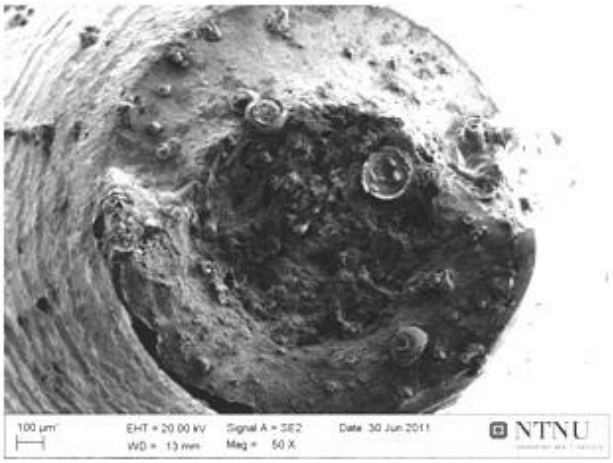

a)

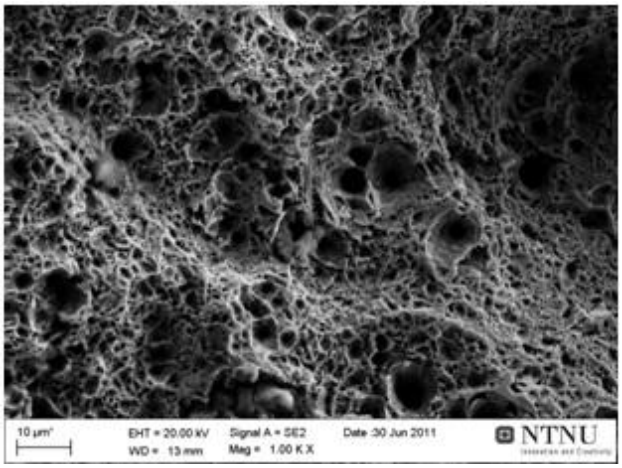

b)

Figure 50. a) Macroscopic view of the tensile specimen *CorTest15.s(free)* of the fractured chain at 50x. b) Fractographic photo of the center of sample *CorTest17.s(free)* at 1000x with dimples.

The fracture surface contains dimples indicating a ductile fracture.

CorTest18.s(galv)

Specimen *CorTest17.s(free)* was first subjected to constant load equivalent to 100% of its tensile strength/ fractured load. After 70hours is was discovered the specimen load was too low. It was decided to increase the load to the correct level. While increasing the load, the specimen fractured.

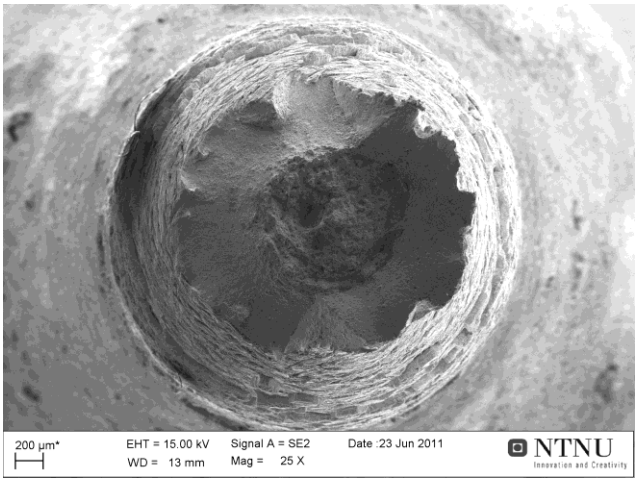

a)

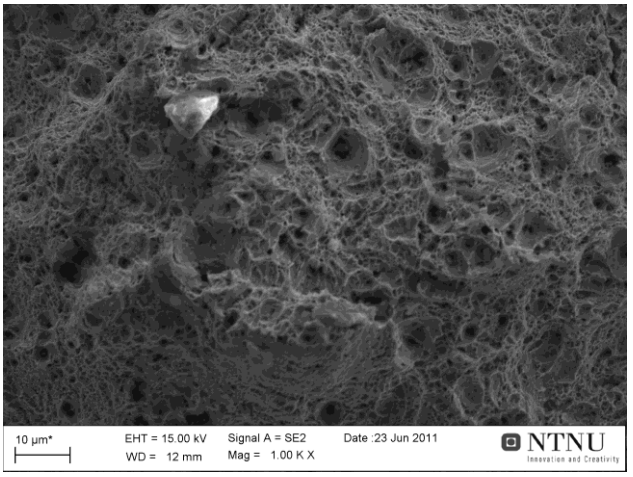

b)

Figure 51. a) Macroscopic view of the tensile specimen CorTest18.s(galv) of the fractured chain at 25x. b) Fractographic photo of the center of sample CorTest18.s(galv)at 1000x with dimples.

The fracture surface contains dimples indicating a ductile fracture.

Attachment B.13 – Microcracks in the SEM

Microcracks in specimens tested at 100% of 1070MPa

Specimen CorTest16.s

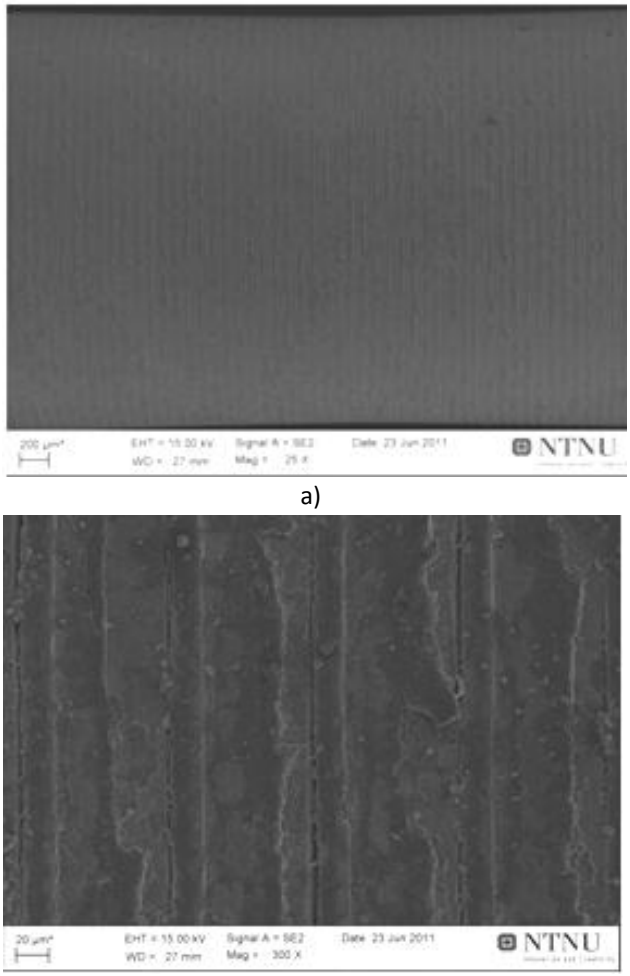

a)

b)

Figure 52. a) Macroscopic view of the tensile specimen *CorTest16.s* of the fractured chain at 25x. b) Several microcracks found in the center of sample *CorTest16.s* at 300x.

Several microcracks were observed on the surface of *CorTest16.s*.

Specimen CorTest12.s.(free)

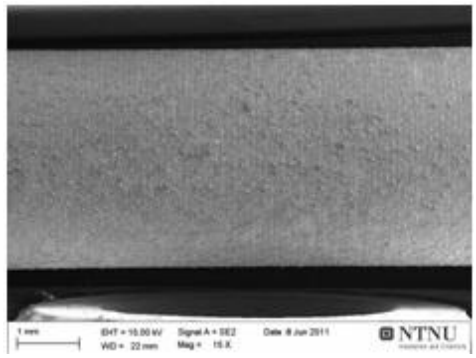

a)

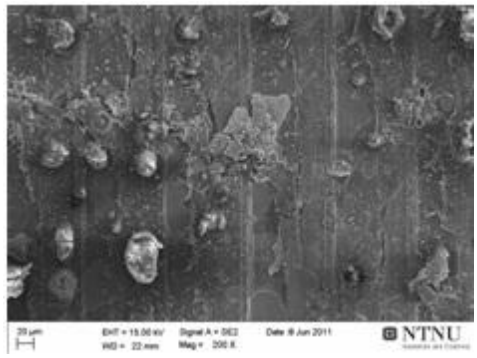

b)

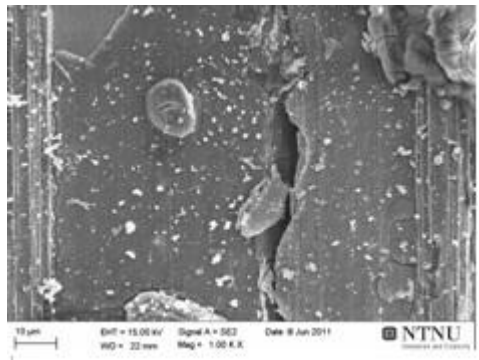

c)

Figure 53. Microcracks examinations in the SEM at; a) 15x, b) 200x and c) 1000x.

Microcracks are oriented along the machining groove at the surface. Corrosion products can be observed on the specimen surface.

Specimen CorTest24.s(galv)

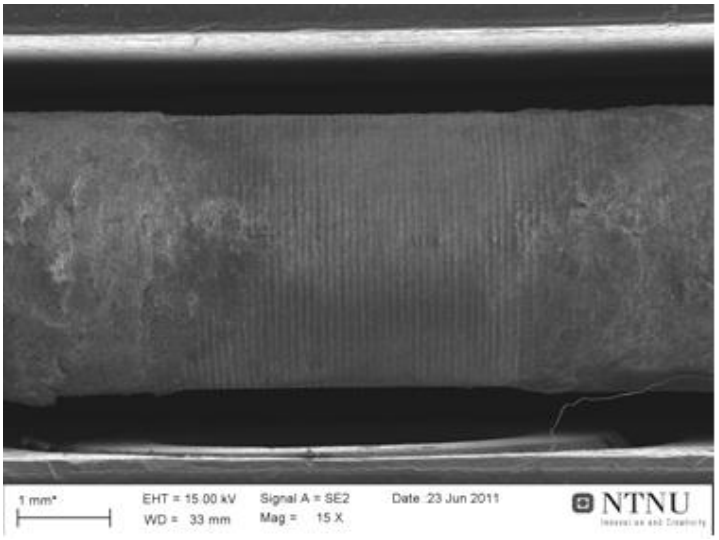

a)

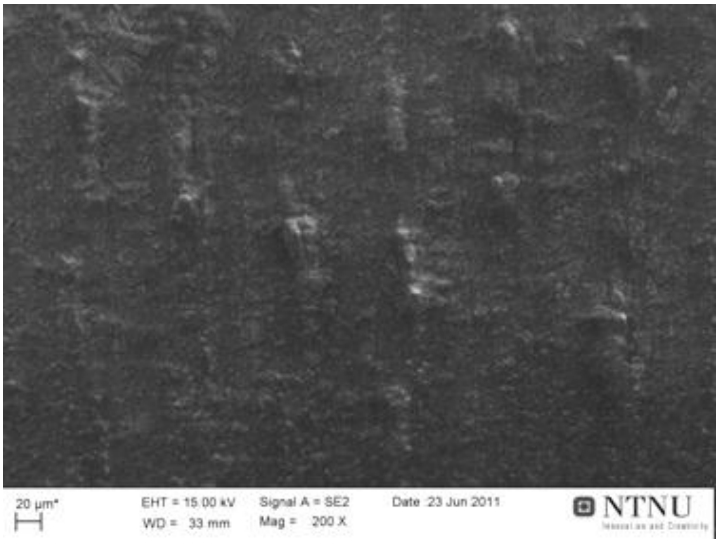

b)

Figure 54. a) Macroscopic view of the damaged area of the HTG specimen *CorTest24.s(galv)* of the fractured chain at 15x. b) The center of *CorTest24.s(galv)* magnified at 200x.

No microcracks were observed on the surface of the "damaged" area of specimen *CorTest24.s(galv)*. No microcracks were observed on the HTG part of the specimen either.

Attachment B.14 – Calculations

The potential, below which the hydrogen reduction reaction can occur, is calculated by inputting known parameters into equation 6, page 13.

At a pH of 6.5 the hydrogen reduction reaction (equation 1, page 8) can occur below the potential E_0. Known values are inserted. The standard electrode potential, E_0^0, of the hydrogen reduction is 0v[6], and *z* is 2:

$$E_0 = 0V - \frac{0.059}{2} \times log \frac{1}{[H^+]^2} = \frac{0.059 \cdot 2}{2} \times log[H^+] = 0.059 \cdot log\ (10^{-pH})$$

$$E_0 = 0.059 \cdot log(10^{-6.5}) = -0.384V$$

E_0 = *-384mV*